

# PPAR $\beta/\delta$ recruits NCOR and regulates transcription reinitiation of *ANGPTL4*

Nathalie Legrand<sup>1</sup>, Clemens L. Bretscher<sup>1</sup>, Svenja Zielke<sup>1</sup>, Bernhard Wilke<sup>1,2</sup>, Michael Daude<sup>3</sup>, Barbara Fritz<sup>4</sup>, Wibke E. Diederich<sup>3,5</sup> and Till Adhikary<sup>1,2,\*</sup>

<sup>1</sup>Department of Medicine, Institute for Molecular Biology and Tumour Research, Centre for Tumour Biology and Immunology, Philipps University, Hans-Meerwein-Strasse 3, 35043 Marburg, Germany, <sup>2</sup>Department of Medicine, Institute for Medical Bioinformatics and Biostatistics, Centre for Tumour Biology and Immunology, Philipps University, Hans-Meerwein-Strasse 3, 35043 Marburg, Germany, <sup>3</sup>Core Facility Medicinal Chemistry, Centre for Tumour Biology and Immunology, Philipps University, Hans-Meerwein-Strasse 3, 35043 Marburg, Germany, <sup>4</sup>Centre for Human Genetics, Universitätsklinikum Giessen und Marburg GmbH, Baldingerstrasse, 35043 Marburg, Germany and <sup>5</sup>Department of Pharmacy, Institute for Pharmaceutical Chemistry, Centre for Tumour Biology and Immunology, Philipps University, Hans-Meerwein-Strasse 3, 35043 Marburg, Germany

Received February 21, 2019; Revised July 20, 2019; Editorial Decision July 24, 2019; Accepted July 28, 2019

## ABSTRACT

In the absence of ligands, the nuclear receptor PPAR $\beta/\delta$  recruits the NCOR and SMRT corepressors, which form complexes with HDAC3, to canonical target genes. Agonistic ligands cause dissociation of corepressors and enable enhanced transcription. *Vice versa*, synthetic inverse agonists augment corepressor recruitment and repression. Both basal repression of the target gene *ANGPTL4* and reinforced repression elicited by inverse agonists are partially insensitive to HDAC inhibition. This raises the question how PPAR $\beta/\delta$  represses transcription mechanistically. We show that the PPAR $\beta/\delta$  inverse agonist PT-S264 impairs transcription initiation by decreasing recruitment of activating Mediator subunits, RNA polymerase II, and TFIIB, but not of TFIIA, to the *ANGPTL4* promoter. Mass spectrometry identifies NCOR as the main PT-S264-dependent interactor of PPAR $\beta/\delta$ . Reconstitution of knockout cells with PPAR $\beta/\delta$  mutants deficient in basal repression results in diminished recruitment of NCOR, SMRT, and HDAC3 to PPAR target genes, while occupancy by RNA polymerase II is increased. PT-S264 restores binding of NCOR, SMRT, and HDAC3 to the mutants, resulting in reduced polymerase II occupancy. Our findings corroborate deacetylase-dependent and -independent repressive functions of

HDAC3-containing complexes, which act in parallel to downregulate transcription.

## INTRODUCTION

PPAR $\beta/\delta$  (peroxisome proliferator activated receptor  $\beta/\delta$ ) is a type II nuclear receptor which constitutively binds to DNA as an obligate heterodimer with a retinoid X receptor (RXR). Its target genes function in lipid and glucose metabolism and also in inflammation (1,2). In the absence of ligands, the PPAR $\beta/\delta$ -RXR heterodimer represses its canonical target genes (1) via the recruitment of corepressors (3) such as NCOR (nuclear receptor corepressor)- and SMRT (silencing mediator of retinoid and thyroid hormone receptors)-containing complexes (4–6). Both corepressor complexes harbour the catalytic subunit histone deacetylase 3 (HDAC3) (7,8), whose activity requires binding to NCOR or SMRT (9). Several fatty acids and their derivatives act as endogenous PPAR $\beta/\delta$  agonists (10–13). Agonistic ligands cause dissociation of corepressors from the nuclear receptor at ligand-regulated target genes, while synthetic inverse agonists recently developed in our group lead to enhanced corepressor recruitment (5,14–16). An important PPAR target gene is *ANGPTL4* (*angiopoietin-like 4*), a regulator of lipid metabolism, angiogenesis, wound healing, and metastasis (15,17). Basal repression of *ANGPTL4* and augmented repression in the presence of inverse agonists are largely insensitive to trichostatin A (15), an inhibitor of class I and II HDACs, suggesting an HDAC-independent repression mechanism. Induction of *ANGPTL4* transcription by activating stimuli is efficiently suppressed by PPAR $\beta/\delta$  inverse agonists, and

\*To whom correspondence should be addressed. Tel: +49 6421 28 66773; Fax: +49 6421 28 68923; Email: adhikary@imt.uni-marburg.de  
Present addresses:

Clemens L. Bretscher, German Cancer Research Centre (DKFZ), Laboratory of Oncolytic Virus Immuno-Therapeutics, Heidelberg, Germany.  
Svenja Zielke, Institute for Experimental Cancer Research in Pediatrics, Komturstr. 3a, 60528 Frankfurt, Germany.

this coincides with decreased binding of RNA polymerase II (RNAPII) (15). Agonists alleviate basal repression, and transcription is induced synergistically with other activating stimuli (18,19).

The preinitiation complex (PIC) is comprised of the general transcription factors (GTFs; TFIIA, TFIIB, TFIID, TFIIE, TFIIIF, and TFIIH), the Mediator complex, and RNAPII (20–24). Its formation is a prerequisite and a rate-limiting process for RNAPII-dependent transcription. After promoter clearance by the polymerase, additional rounds of transcription are initiated from the scaffold complex, which contains a subset of general transcription factors that remain bound to the promoter. It was shown that reinitiation of transcription from an immobilized template requires reincorporation of TFIIB, TFIIIF, and RNAPII into the scaffold (25), yielding a reinitiation complex (RIC). The re-use of remaining promoter-bound GTFs supersedes the need for recurrent PIC formation and thus enables high-level transcription. Moreover, dephosphorylation of the carboxyterminal domain (CTD) of the large subunit of RNAPII after termination allows for RNAPII recycling, which is enhanced by proximity of the transcription start site (TSS) and the terminator (26). TFIIB is necessary for the formation of these gene loops (27–29). *In vitro*, human Mediator facilitates TFIIB and RNAPII recruitment (30), and its kinase module regulates reinitiation (31). Little is known about the regulation of transcription reinitiation *in vivo* (32).

In the present study, we investigated the mechanism of transcriptional repression by PPAR $\beta/\delta$  inverse agonists in human cell lines. Due to its particularly strong regulation by PPAR ligands in different cell types (1,13,15,18,33–35) and pronounced crosstalk with effector transcription factors of signalling pathways such as HIF and TGF $\beta$ , the *ANGPTL4* gene served as a model locus for mechanistic studies by us and by others (15,18,19,35,36). To analyse how PPAR $\beta/\delta$  inverse agonists counteract transcriptional induction of *ANGPTL4*, we used TGF $\beta$  as a defined activating stimulus. Our data show that inverse agonists interfere with TGF $\beta$ -dependent recruitment of TFIIB, RNAPII, and activating Mediator subunits to the *ANGPTL4* promoter, while binding of the scaffold GTFs TFIIA and TFIIH is unchanged. This suggests an impairment of the Mediator-TFIIB recruitment step, affecting RNAPII binding and reinitiation. The binding pattern of RNAPII at the *ANGPTL4* locus in the presence of an inverse agonist is similar to the pattern elicited by the transcription initiation inhibitor triptolide. We identify NCOR as the main ligand-dependent interactor of PPAR $\beta/\delta$  in the presence of the inverse agonist PT-S264. Strikingly, PT-S264-dependent repression is partially insensitive to both trichostatin A (a non-selective HDAC inhibitor) and also to apicidin, an HDAC3-selective inhibitor. Expression of PPAR $\beta/\delta$  mutants in PPAR $\beta/\delta$  knockout cells identified amino acid residues required for basal repression. These PPAR $\beta/\delta$  mutants revealed diminished NCOR, SMRT, and HDAC3 binding to PPAR target genes in the basal state, concomitant with increased RNAPII binding. Recruitment of NCOR, SMRT, and HDAC3 was restored by the inverse agonist, as was RNAPII loss and repression of transcription. Repression of PPAR target genes by these

mutant receptors was largely insensitive to HDAC inhibition. Our data show that chromatin-bound NCOR and SMRT complexes downregulate transcription reinitiation, and possibly initiation, via both deacetylase-dependent and -independent mechanisms.

## MATERIALS AND METHODS

### Antibodies

The following antibodies were used in this study: HDAC3, Santa Cruz no. sc-11417, rabbit polyclonal, Chromatin immunoprecipitation (ChIP), RRID AB\_2118706; LDH, Santa Cruz no. sc-33781, rabbit polyclonal, immunoblot, RRID AB\_2134947; MED1, Santa Cruz no. sc-8998, rabbit polyclonal, ChIP, RRID AB\_2144021; MED13L, Bethyl no. A302-420A, rabbit polyclonal, ChIP, RRID AB\_1907303; MED26, Santa Cruz no. sc-48776, rabbit polyclonal, ChIP, RRID AB\_782277; NCOR, Abcam no. ab24552, rabbit polyclonal, ChIP, RRID AB\_2149005; NCOR, Bethyl no. A301-145A, rabbit polyclonal, ChIP, RRID AB\_873085; NCOR, Thermo no. PA1-844A, rabbit polyclonal, immunoblot, RRID AB\_2149004; IgG fraction, Sigma no. I5006, rabbit polyclonal, ChIP, RRID AB\_1163659; PPAR $\alpha$ , Santa Cruz no. sc-9000, rabbit polyclonal, ChIP and immunoblot, RRID AB\_2165737; PPAR $\beta/\delta$ , Santa Cruz no. sc-7197, rabbit polyclonal, ChIP, RRID AB\_2268420; PPAR $\beta/\delta$ , Santa Cruz no. sc-74517, mouse monoclonal, immunoblot, RRID AB\_1128604; PPAR $\gamma$ , Santa Cruz no. sc-7196, rabbit polyclonal, ChIP and immunoblot, RRID AB\_654710; RPB1 (RNAPII large subunit) CTD (37), Biologend no. 8WG16, mouse monoclonal, ChIP, RRID AB\_2565554; RPB1 unphosphorylated CTD (38), Ascension no. 1C7, rat monoclonal, ChIP, RRID AB\_2631402; RPB1 Ser5-phosphorylated CTD (39), Ascension no. 3E8, rat monoclonal, ChIP, RRID AB\_2631404; RPB1 Ser2-phosphorylated CTD (39), Ascension no. 3E10, rat monoclonal, ChIP, RRID AB\_2631403; RPB1 NTD, Santa Cruz no. sc-899, rabbit polyclonal, ChIP, RRID AB\_632359; RPB1 NTD, Santa Cruz no. sc-9001, rabbit polyclonal, ChIP, RRID AB\_2268548; RXR, Santa Cruz no. sc-774, rabbit polyclonal, ChIP, RRID AB\_2270041; SMRT, Abcam no. ab24551, rabbit polyclonal, ChIP, RRID AB\_2149134; TBLR1, Novus no. NB600-270, rabbit polyclonal, ChIP, RRID AB\_10001343; TBP, Santa Cruz no. sc-273, rabbit polyclonal, ChIP, RRID AB\_2200059; TFIIA, Santa Cruz no. sc-25365, rabbit polyclonal, ChIP, RRID AB\_2116529; TFIIB, Santa Cruz no. sc-225, rabbit polyclonal, ChIP, RRID AB\_2114380; TFIIH, Santa Cruz no. sc-293, rabbit polyclonal, ChIP, RRID AB\_2262177.

### Cell culture and treatment

$\phi$ NX cells (40) were cultivated in Dulbecco's modified Eagle's medium with 10% fetal bovine serum (FBS). MDA-MB231-*luc2* and Caki-1 cells were cultivated in McCoy's 5A medium with 10% FBS. The compound or compounds were added for 6 h (expression analyses) or 30 min (ChIP assays) to the cultures. Control populations were supplied with an equivalent volume of solvent (dimethyl sulfoxide (DMSO) for low molecular weight compounds, phosphate-

buffered saline with 0.1 % (w/v) fatty acid free bovine serum albumin (BSA) for TGF $\beta$ ).

### Compounds

Name	supplier	cat. no. or citation
Apicidin	Cayman	10 575
Blasticidin	Fisher Scientific	10 648 203
DRB	Cayman	10 010 302
Flavopiridol	Cayman	10 009 197
L165,041	Tocris	1856
Pioglitazone	Adipogen	AG-CR1-0067
PT-S264	in-house	(16)
ST247	in-house	(46)
TGF $\beta$	Merck	616 450
TGF $\beta$	Sigma	T5300
Trichostatin A	Appllichem	A7812
Triptolide	Cayman	11973
Wy-14643	Cayman	70 730

### Genetic deletion and stable transfection

Vectors for parallel expression of a guide RNA and the Cas9 nuclease were obtained from Santa Cruz Biotechnology. The sequences targeting the *PPARD* coding region were TC GTACGATCCGCATGAAGC (i), CCCTGTGCAGCTATCCGTTT (ii) and AACACTCACCGCCGTGTGGC (iii). MDA-MB231-*luc2* cells were transfected using Lipofectamine 2000 (Life Technologies) according to the manufacturer's instructions with the guide/Cas9 expression vectors together with pMSCVbsd (41) for selection of transfected cells. After 4 h, the cells were supplemented with fresh medium, and blasticidin was added after 30 h at a concentration of 10  $\mu$ g/ml. After 10 days, single cells were seeded using limiting dilution in cell-free medium conditioned by the parental cell line. Wells with more than one colony were terminated. Clones were expanded and screened via RT-qPCR (loss of *ANGPTL4* repression by PT-S264) and immunoblotting against PPAR $\beta$ / $\delta$ . The 2B3 clone was transfected with pWZLneo-ecoR (42). After 24 h, the cells were selected with 500  $\mu$ g/ml G418 for 14 days.

### *PPARD* expression vectors

The retroviral vector pMSCVbsd (41) was used to clone the *PPARD* cDNA into the BglIII and XhoI sites. Terminal deletions were introduced via polymerase chain reaction (PCR) with specific primers, and the fragment was reinserted into the empty pMSCVbsd vector. Alterations in the cDNA sequence were introduced with site-directed mutagenesis. All plasmid preparations used for retroviral transduction were validated by sequencing of the entire cDNA inserts. Subsequent new plasmid preparations were validated by resequencing. Vectors are available from Addgene.

### Retroviral transduction

For production of ecotropic retroviruses, pMSCVbsd-*PPARD* vectors or the empty vector were transfected into subconfluent  $\phi$ NX-eco packaging cells (40). After 4 h, 7 ml of fresh medium were added. Twenty-four hours later, the supernatant was harvested, centrifuged at 800  $\times$  g, and 3 ml

aliquots were snap frozen. The  $\phi$ NX-eco cells received fresh medium, and a second supernatant was harvested 24 h later. Freshly seeded MDA-MB231-*luc2*-2B3 cells ectopically expressing the ecotropic receptor were incubated with 2 ml of fresh medium, 3 ml of  $\phi$ NX supernatant, and 4  $\mu$ g/ml polybrene for 24 h. Selection was performed with 10  $\mu$ g/ml blasticidin for ten days, and cells were subsequently cultured in the presence of blasticidin.

### RNA isolation, cDNA synthesis and quantitative RT-PCR

Total RNA was isolated with the NucleoSpin RNA kit (Macherey&Nagel, no. 740955) according to the manufacturer's instructions; the DNase digestion and desalting steps were omitted. Complementary DNA synthesis was carried out with the iScript cDNA Synthesis Kit (Bio-Rad, no. 170-8891SP) according to the manufacturer's instructions with 500 ng of purified RNA per sample in 20  $\mu$ l. Quantitative PCR analyses were performed in three technical replicates per sample using Absolute SYBR Green master mix (Thermo Scientific, no. AB-1158B) in a total reaction volume of 10  $\mu$ l in M $\times$ 3000p and Mx3005 thermocyclers (Agilent). Prior to PCR, cDNA samples were diluted 1:10, and 4.75  $\mu$ l were used per reaction. The *RPL27* transcript was used for normalization. RT-qPCR was carried out with primer concentrations of 250 nM each. The primer sequences are available in Supplementary Table S1. Ct values were normalized to the *RPL27* transcript; to retain information about *ANGPTL4* expression levels, the mean *RPL27* Ct value of all samples in the respective assay was added back where suitable.

### Chromatin immunoprecipitation (ChIP)-qPCR

ChIP was essentially performed as described previously (43,44). Fixation was performed with 1 % formaldehyde in media for 10 min at room temperature followed by quenching with 125 mM glycine for 5 min. Cells were lysed in buffer L1 (5 mM PIPES pH 8.0, 85 mM KCl, 0.5 % (v/v) NP40, protease inhibitor mix (Sigma, no. P8340, 1:1000) for 20–40 min on ice. Nuclei were resuspended in ChIP RIPA buffer (10 mM Tris-HCl pH 7.5, 150 mM NaCl, 1 % (v/v) NP40, 1 % (w/v) sodium deoxycholate, 1 mM ethylenediaminetetraacetic acid (EDTA)) supplemented with 1:1000 protease inhibitor mix (Sigma), incubated on ice for 10–20 min and sheared with a Branson S250D Sonifier (Branson Ultrasonics) using a microtip in 1 ml aliquots in 15 ml conical tubes. 40–52 pulses of 1 s, 4 s pause, 20 % amplitude were applied with cooling of the sample in an ice-ethanol mixture or in a 15 ml tube cooler (Active Motif, no. 53077). A 15 min 17 000  $\times$  g supernatant was precleared with 10  $\mu$ g of IgG coupled to 100  $\mu$ l of blocked sepharose slurry (see below) for 45 min at 4  $^{\circ}$ C with agitation. IP was carried out with 300  $\mu$ l of precleared chromatin, equivalent to 6–8  $\times$  10<sup>6</sup> cells. ChIP was performed using 4  $\mu$ g of antibody per sample. For precipitation, a mixture of protein A and protein G sepharose (GE Healthcare life sciences, no. 1752800 and no. 1706180) or pure protein A sepharose (Zymed) was washed twice with ChIP RIPA buffer and blocked with 1 g/l BSA and 0.4 g/l sonicated salmon sperm DNA (Life Technologies no. 15632011) overnight. A total of 50  $\mu$ l of blocked

bead slurry (1:1 volume ratio with liquid phase) were used per IP. Samples were washed once in buffer I (20 mM Tris pH 8.1; 150 mM NaCl; 1% (v/v) Triton X-100; 0.1% (w/v) sodium dodecyl sulphate (SDS); 2 mM EDTA), once in buffer II (20 mM Tris pH 8.1; 500 mM NaCl; 1% (v/v) Triton X-100; 0.1% (w/v) SDS; 2 mM EDTA), twice in buffer III (10 mM Tris pH 8.1; 250 mM LiCl; 1% (v/v) NP40; 1% (w/v) sodium deoxycholate; 1 mM EDTA) on ice, and twice in Qiagen buffer EB (10 mM Tris pH 8.0; no. 19086) at room temperature. Immune complexes were eluted twice with 100 mM NaHCO<sub>3</sub> and 1% (w/v) SDS under agitation. Eluates were incubated overnight at 65 °C after adding 10 µg of RNase A and 20 µg of proteinase K in the presence of 180 mM NaCl, 35 mM Tris-HCl pH 6.8 and 9 mM EDTA. An input sample representing 1% of the chromatin used per IP was reverted in parallel. Samples were purified using the Qiagen PCR purification kit according to the manufacturer's instructions. ChIP-qPCR was performed in three technical replicates per sample with the Absolute SYBR Green master mix (Thermo Scientific, no. AB-1158B) in Mx3000p and Mx3005 thermocyclers (Agilent). Quantitative PCR was carried out with primer concentrations of 250 nM each. The primer sequences are available in Supplementary Table S2.

### ChIP-mass spectrometry (ChIP-MS)

Two technical replicates each were performed by Active Motif Epigenetic Services according to a published protocol (45) from the following MDA-MB231-*luc2* samples: IgG, PT-S264 treatment (0.3 µM); α-PPARβ/δ, PT-S264 treatment (0.3 µM); α-PPARβ/δ, L165,041 treatment (1.0 µM). The unspecific IgG pool from rabbit was obtained from Sigma-Aldrich (no. I5006), the PPARβ/δ antibody from Santa Cruz Biotechnology (sc-7197, rabbit polyclonal). Candidate proteins were filtered with scaffold Viewer 4.8.3 (Proteome Software) according to the following criteria: at least two unique peptides in total and a maximum of two unique peptides each in the negative control replicates (IgG). The protein and the peptide thresholds were each set to 80%.

## RESULTS

### PPARβ/δ inverse agonists interfere with formation of an initiation complex

PT-S264 is an inverse PPARβ/δ agonist with improved repressive properties and stability (16). We first tested whether it affects initiation complex formation like the previously used inverse agonist ST247 (46), which reduces RNAPII binding to the *ANGPTL4* promoter (15). TGFβ is a strong inducer of *ANGPTL4* transcription in human cells (18). Treatment with PT-S264 strongly reduced RNAPII (large subunit RPB1) binding to the *ANGPTL4* TSS as shown by scanning ChIP-qPCR using closely spaced primer pairs (Figure 1A) both in the presence and in the absence of TGFβ in Caki-1 cells. We used the 8WG16 antibody, which in our hands detects total RNAPII with superior specificity to other RNAPII antibodies (Supplementary Figure S1). The binding pattern of RNAPII in PT-S264-treated cells is similar to the binding pattern observed in cells

treated with the transcription initiation inhibitor triptolide, which however is more effective in reducing RNAPII binding compared to PT-S264 (upper panels of Figure 1A). In contrast, treatment of the cells with the CDK9 inhibitors DRB and flavopiridol, which interfere with elongation, does not prevent TGFβ-induced RNAPII accumulation at the TSS (blue and green lines in the lower panels of Figure 1A). This indicates that PT-S264 prevents RNAPII recruitment to the *ANGPTL4* promoter in a manner similar to the effect of triptolide. Taken together, these observations show that PT-S264 impinges on transcription initiation of *ANGPTL4*. Notably, ChIP-qPCR data obtained with antibodies against the RPB1 CTD phosphorylated at serine 5 (initiating RNAPII) or serine 2 (elongating RNAPII) do not support an effect of PT-S264 on serine 2 phosphorylation when taking total RNAPII enrichment into account (Supplementary Figure S1), which again implies that the inverse agonist diminishes RNAPII recruitment and furthermore argues against an effect of PT-S264 on RPB1 CTD phosphorylation. We therefore conclude that the formation of an initiation complex is affected by PT-S264.

In order to clarify how PT-S264 interferes with RNAPII recruitment, we performed further experiments with the Caki-1 line. These cells highly express *ANGPTL4* (15) and hence allow for ChIP-based detection of GTFs at the endogenous locus. To address which step of initiation complex formation is affected, we measured the occupancy of GTFs at the *ANGPTL4* TSS in the presence or in the absence of PT-S264. Binding of TFIIB and RNAPII is reduced upon treatment with PT-S264 compared to the control. However, the occupancy of TFIIA is not altered (Figure 1B), suggesting that the repressive mechanism affects the transition from the scaffold complex to the RIC. PIC formation may be impaired too, which cannot be inferred from these data obtained after short-term treatment. The effect of PT-S264 is PPAR-dependent, as TFIIB and RNAPII binding remain unchanged at the TSS of *TSC22D3*, which is not a PPAR target. In the presence of TGFβ, TFIIB binding to the *ANGPTL4* TSS is increased, and this is counteracted by PT-S264 (Figure 1C).

The Mediator complex facilitates the rate-limiting step of TFIIB recruitment, and both Mediator and TFIIB are necessary for RNAPII binding in a reconstituted human transcription system (30) as well as in *Saccharomyces cerevisiae* *in vivo* (47). Initial ChIP-qPCR experiments after treatment with the previously used inverse agonist ST247 show that both TFIIH, another GTF present in the scaffold, and MED1 (Mediator subunit 1) bind to the *ANGPTL4* TSS after TGFβ treatment. However, in the presence of the inverse agonist ST247, MED1 recruitment is blocked (Supplementary Figure S2); TBP ChIP data were not conclusive and show an enrichment pattern similar to MED1. The TFIIA and TFIIH ChIPs show that inverse agonists do not generally block recruitment of PIC components. This led to the hypothesis that PPARβ/δ inverse agonists affect Mediator binding to the promoter. Scanning ChIP-qPCR analyses of Caki-1 cells treated with PT-S264, TGFβ, or both show that PT-S264 counteracts TGFβ-stimulated recruitment of MED1 (Figure 2A) and MED26 (Figure 2B) around the *ANGPTL4* TSS. Both MED1 and MED26 are enriched in forms of Mediator that are permissive for tran-

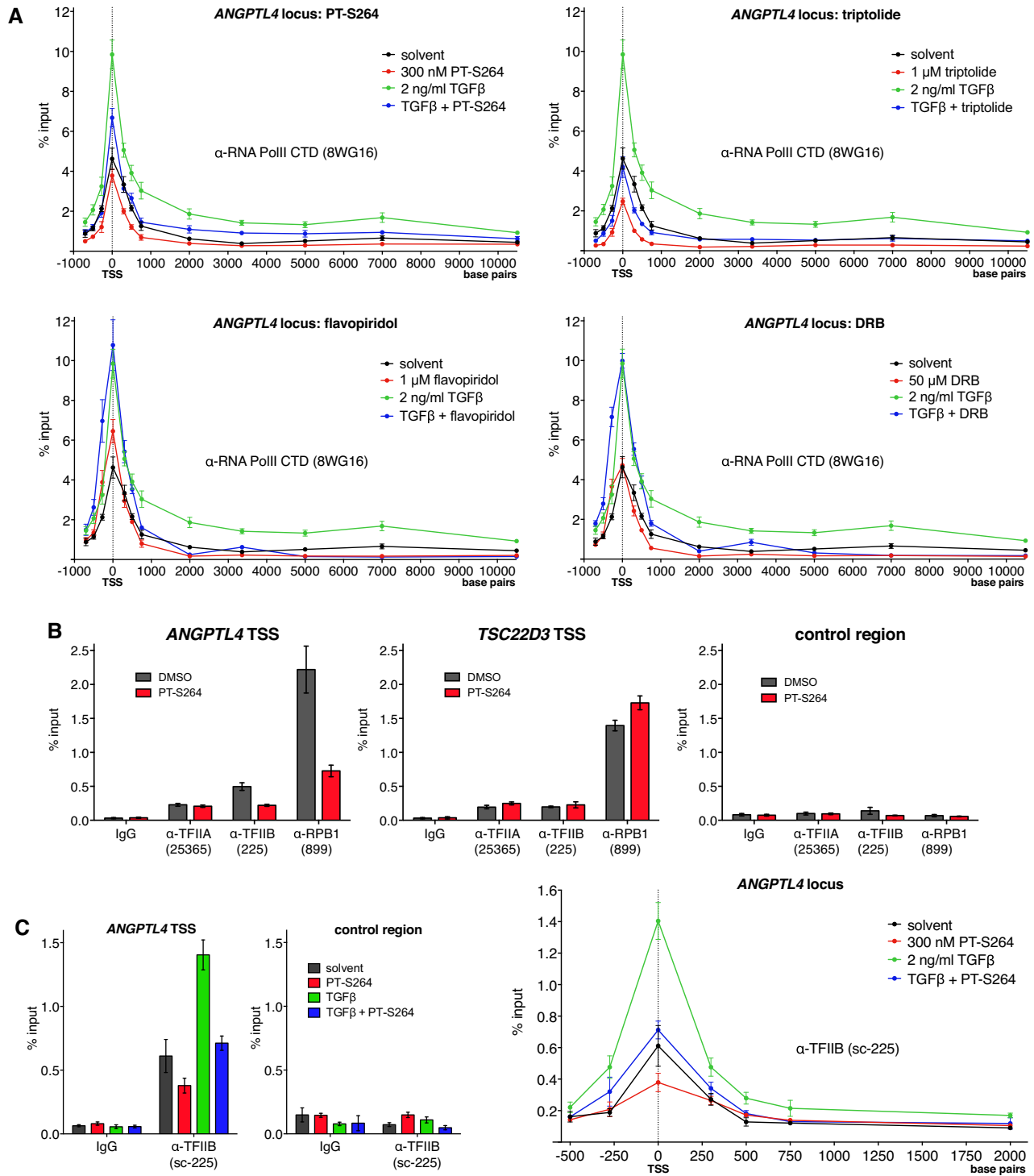


**Figure 1.** PPAR $\beta/\delta$  inverse agonists suppress transcription initiation of *ANGPTL4* and recruitment of TFIIB to a scaffold complex. Caki-1 cells were treated for 30 min as indicated and subjected to ChIP-qPCR analysis. (A) Scanning ChIP-qPCR of the *ANGPTL4* locus. An antibody against the CTD of the large subunit of RNAPII was used. (B) Binding of TFIIA, TFIIB and RPB1 at the *ANGPTL4* and *TSC22D3* TSSs. (C) TFIIB binding at the *ANGPTL4* TSS in the presence of TGF $\beta$ , PT-S264, or both. The right panel shows scanning ChIP around the *ANGPTL4* TSS from the same samples. Commercially available antibodies are denominated by the terms in parentheses. Means and standard deviations of three technical replicates from representative ChIP assays are plotted.

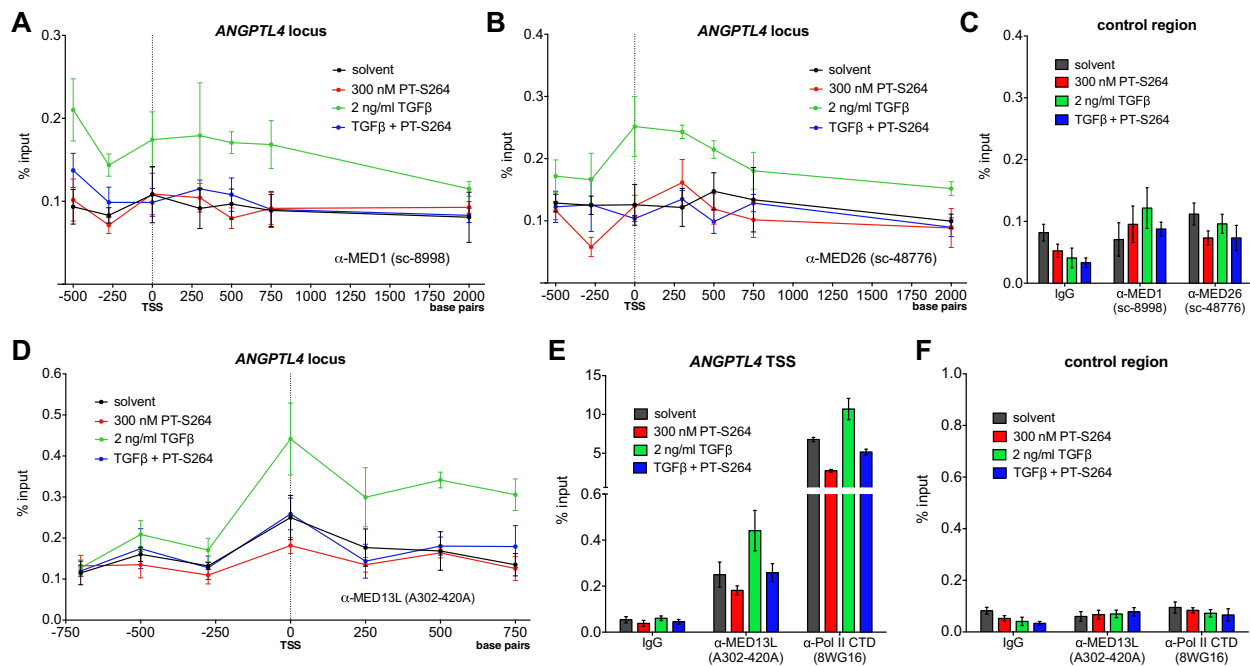


**Figure 2.** PPAR $\beta/\delta$  inverse agonists prevent TGF $\beta$ -stimulated recruitment of Mediator subunits to the *ANGPTL4* promoter. Caki-1 cells were treated for 30 min as indicated and subjected to scanning ChIP-qPCR analysis with primer pairs that amplify regions close to the TSS of *ANGPTL4*. Antibodies against MED1(A), MED26 (B) and MED13L (D) were used. Panels (C and F) show ChIP-qPCR data from these samples using a negative control region primer pair. In (E) RNAPII binding is shown as an additional control. Commercially available antibodies are denominated by the terms in parentheses. Means and standard deviations of three technical replicates from representative ChIP assays are plotted.

scription (48–50). Since the Mediator kinase module is detected at promoters in metazoans (51), we performed additional scanning ChIP across the *ANGPTL4* TSS with an antibody against MED13L, a Mediator subunit that resides in the kinase module in the presence of MED26 (52). Recruitment of MED13L upon stimulation with TGF $\beta$  but not after simultaneous treatment with the inverse agonist PT-S264 (Figure 2D) is detected in the same manner as MED1 (Figure 2A and Supplementary Figure S2), MED26 (Figure 2B), TFIIB (Figure 1B), and RNAPII (Figure 1A and Supplementary Figure S1). At the promoter of *PAIL*, which is a TGF $\beta$  target gene but not a PPAR target gene, TGF $\beta$ -stimulated recruitment of MED1 and MED26 was not impaired by PT-S264 (Supplementary Figure S3). Taken together, our data suggest that MED1, MED13L, and MED26 binding occur in a transcriptionally permissive state induced by TGF $\beta$ , which is prevented in the presence of PT-S264. We conclude that PPAR $\beta/\delta$  inverse agonists perturb transcription initiation at the *ANGPTL4* TSS by interfering with TFIIB–RNAPII recruitment to promoter-bound GTFs, and this is achieved by preventing recruitment of MED1, MED13L, and MED26 to the promoter.

### PT-S264 augments NCOR binding to PPAR $\beta/\delta$

We previously found that depletion of NCOR by RNAi alleviates basal repression to the same extent as PPAR $\beta/\delta$  depletion but does not prevent repression by an inverse agonist (15). However, RNAi-mediated partial depletion may not suffice for full loss of function, especially if the affinity of PPAR $\beta/\delta$  binding to NCOR is considerably high

in the presence of an inverse agonist. To identify candidate repressors in an unbiased approach, ChIP-mass spectrometry (ChIP-MS) according to the RIME (rapid immunoprecipitation and mass spectrometry of endogenous proteins) protocol (45) was performed with an antibody against PPAR $\beta/\delta$ . We used chromatin from MDA-MB231-*luc2* cells, in which PPAR $\beta/\delta$  target gene repression by inverse agonists is particularly strong (Supplementary Figure S2 and (15)). PPAR $\beta/\delta$  and RXR were robustly identified both in the presence of the inverse agonist PT-S264 and the agonist L165,041 (see Table 1). Importantly, NCOR (encoded by the *NCOR1* gene) and SMRT (encoded by the *NCOR2* gene) were identified as interactors only in the presence of PT-S264 but not in the presence of L165,041. Other known transcriptional repressors were not detected. The NCOR2 protein cluster revealed 15 and 7 unique peptides for NCOR after treatment with PT-S264 in the two technical replicates, while only 4 and 3 peptides were identified for SMRT. This finding may indicate that NCOR binding to PPAR $\beta/\delta$  is dominant over SMRT binding in MDA-MB231-*luc2* cells in the presence of PT-S264. Of note, TBL1XR1, a subunit of NCOR and SMRT complexes (7), was also only detected in the presence of PT-S264 but not in the presence of L165,041. Other NCOR and SMRT complex subunits such as HDAC3 were not detected. This could be due to insufficient sensitivity, the destructive nature of chromatin sample preparation, or both.

Next, we measured NCOR binding to the PPAR $\beta/\delta$  binding sites (PPREs) of the target genes *ANGPTL4* and *PDK4* (1) in MDA-MB231-*luc2* cells in the presence and in the absence of PT-S264 by ChIP-qPCR using two differ-

**Table 1.** PPAR $\beta/\delta$  interactors in the presence of the inverse agonist PT-S264 or the agonist L165,041 (RIME ChIP-MS analysis)

Protein or cluster	Gene(s)	IgG PT-S264	$\alpha$ -PPAR $\beta/\delta$ PT-S264	$\alpha$ -PPAR $\beta/\delta$ L165,041	diff. count
Neuropathy target esterase	<i>PNPLA6</i>	0	36	41	-5
Envoplakin	<i>EVPL</i>	0	32	24	8
Periplakin	<i>PPL</i>	0	20.5	10.5	10
Cytospin-A	<i>SPECC1L</i>	0.5	16	22.5	-6.5
Nuclear receptor corepressor 2	<b><i>NCOR1, NCOR2</i></b>	0	14.5	0	14.5
Inorganic pyrophosphatase 2, mitochondrial	<i>PPA2</i>	0	14.5	14	0.5
Kinesin-like protein KIF15	<i>KIF15</i>	0.5	11	5.5	5.5
Peroxisome proliferator-activated receptor $\delta$	<b><i>PPARD</i></b>	0	10	16	-6
2-hydroxyacyl-CoA lyase 1	<i>HACL1</i>	0	10	12	-2
Inositol 1,4,5-trisphosphate receptor type 2	<i>ITPR2</i>	0	9.5	5	4.5
BAG family molecular chaperone regulator 3	<i>BAG3</i>	0	8.5	6.5	2
Retinoid X receptor RXR- $\beta$	<b><i>RXR<math>\beta</math>, RXRA</i></b>	0	8	14.5	-6.5
Myotubularin-related protein 12	<i>MTMR12</i>	0	8	5.5	2.5
Zinc finger protein ZPR1	<i>ZPR1</i>	0	7	7	0
TBC1 domain family member 2A	<i>TBC1D2</i>	0.5	6	4	2
Melanoma inhibitory activity protein	<i>MIA3</i>	0	5.5	2	3.5
Nuclear distribution protein nudE-like 1	<i>NDEL1, NDE1</i>	0	5.5	4	1.5
GTPase-activating protein and VPS9 domain-cont. 1	<i>GAPVD1</i>	0	5.5	2	3.5
Zinc finger and BTB domain-containing 9	<i>ZBTB9</i>	0.5	4.5	3.5	1
Membrane-assoc. progesterone receptor component 2	<i>PGRMC2</i>	0	4	2	2
Protein kinase C $\delta$ -binding protein	<i>PRKCDBP</i>	1	4	3.5	0.5
Complement C4-A	<i>C4A</i>	0	3.5	3.5	0
Non-specific lipid-transfer protein	<i>SCP2</i>	1	3	0	3
Ig $\gamma$ -2 chain C region	<i>IGHG2</i>	2	3	1	2
5'-3' exoribonuclease 1	<i>XRNI</i>	0	2.5	5	-2.5
MIA SH3 domain ER export factor 2	<i>MIA2/CTAGE5</i>	0	2.5	0	2.5
m7GpppX diphosphatase	<i>DCPS</i>	0	2.5	3.5	-1
EF-hand calcium-binding domain-containing prot. 4A	<i>CRACR2B</i>	0	2.5	2.5	0
Complement C3	<i>C3</i>	0	2	0	2
FGFR1 oncogene partner	<i>FGFR1OP</i>	0	2	0.5	1.5
E3 ubiquitin-protein ligase TRIM4	<i>TRIM4</i>	1	2	1	1
3-ketoacyl-CoA thiolase, peroxisomal	<i>ACAA1</i>	0	1.5	0.5	1
Transducin- $\beta$ like 1 X-linked receptor 1	<b><i>TBL1XR1</i></b>	0	1.5	0	1.5
Importin subunit $\alpha$ -1	<i>KPNA2</i>	1	1.5	0.5	1
Eukaryotic translation initiation factor 5	<i>EIF5</i>	1.5	1	0	1
E3 ubiquitin-protein ligase RFWD2	<i>RFWD2</i>	0	0	2	-2

The numbers indicate the mean unique peptide count from two technical replicates each. The difference count is peptides(PT-S264)–peptides(L165,041) for the cognate IPs ( $\alpha$ -PPAR $\beta/\delta$ ). An IgG fraction from non-immunized rabbits served as a negative control. The gene names of the antibody target (*PPARD*) and known interactors are printed in boldface.

ent antibodies. In agreement with ChIP-MS data, NCOR is present at the *ANGPTL4* PPREs. Interestingly, we find increased binding of NCOR after treatment with the inverse agonist PT-S264 both in the presence and in the absence of TGF $\beta$  (Figure 3A). Further ChIP-qPCR analyses of several NCOR and SMRT complex subunits are in line with the ChIP-MS results, showing increased recruitment to the PPAR $\beta/\delta$  binding site of *ANGPTL4* in the presence of PT-S264 and decreased recruitment in the presence of L165,041 (Figure 3B). This includes PT-S264-dependent recruitment of HDAC3, which is clearly expressed in these cells (15).

In Caki-1 cells, *ANGPTL4* expression is modulated by L165,041 and PT-S264 in the same manner as in MDA-MB231-*luc2* cells; the amplitude of the effects is weaker in Caki-1, while expression in the basal state is considerably higher (Supplementary Figure S3). Increased NCOR recruitment to the *ANGPTL4* PPREs is also observed in Caki-1 cells upon treatment with PT-S264 (Supplementary Figure S4). Due to its marked contribution to basal repression (15) and its enhanced recruitment to chromatin-bound PPAR $\beta/\delta$  in the presence of PT-S264, we postulate that NCOR mediates downregulation of *ANGPTL4* by

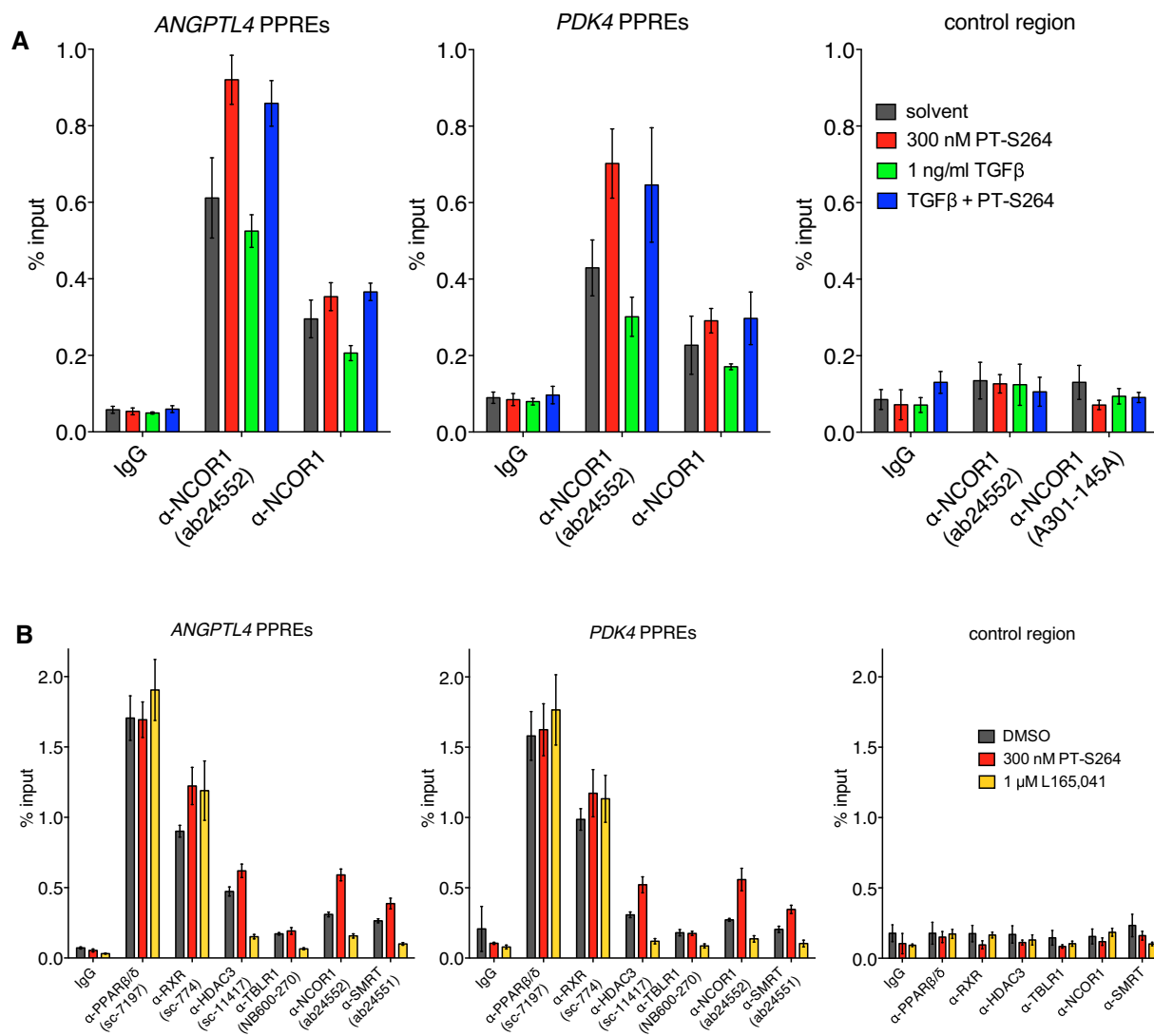


**Figure 3.** NCOR and SMRT complex subunits are recruited to PPAR $\beta/\delta$  in the presence of PT-S264. MDA-MB231-*luc2* cells were treated as indicated for 30 min, and ChIP-qPCR was performed with antibodies against subunits of HDAC3-containing complexes using primer pairs encompassing the *ANGPTL4* and *PDK4* PPRES (+3500 or -12 200 bp relative to the TSS of the gene, respectively). (A) Binding of NCOR in the presence of 300 nM PT-S264, 1 ng/ml TGF $\beta$ , or both. Two different antibodies against NCOR were used. (B) Binding of PPAR $\beta/\delta$ , RXR, HDAC3, TBLR1, NCOR, and SMRT in the presence of solvent (DMSO), 300 nM PT-S264, or 1  $\mu$ M L165,041. Both panels: representative ChIP data are plotted. Commercially available antibodies are denominated by the terms in parentheses. Values denote means and standard deviations from three technical replicates.

PPAR $\beta/\delta$  in the basal state and in the presence of PPAR $\beta/\delta$  inverse agonists. This raises the question whether the interaction of NCOR and PPAR $\beta/\delta$  is necessary for PT-S264-dependent repression.

#### Generation and characterization of PPAR $\beta/\delta$ knockout clones

To test whether NCOR is functionally important for PT-S264-mediated repression, we tried to disrupt NCOR expression through genetic deletion with the CRISPR-Cas9 system but were repeatedly unable to obtain NCOR knockout clones. We therefore aimed to disrupt NCOR binding to PPAR $\beta/\delta$  through mutations of the receptor as an alternative strategy. As a prerequisite for screening PPAR $\beta/\delta$  mutants, we introduced frameshift muta-

tions to the *PPARD* coding region in MDA-MB231-*luc2* cells using the CRISPR-Cas9 system. Four different PPAR $\beta/\delta$  knockout clones were isolated (2B2, 2B3, 2A3, 2A6; see Supplementary Figure S5A). Neither PPAR $\alpha$  nor PPAR $\gamma$  expression was disrupted in the four clones (Supplementary Figure S5B and C). ChIP-qPCR confirmed the absence of PPAR $\beta/\delta$  at the *ANGPTL4* and *PDK4* loci (Figure 4). Interestingly, binding of PPAR $\alpha$  and PPAR $\gamma$  to the *ANGPTL4* and *PDK4* loci, each of which harbours three adjacent PPRES sequences (1,12,18), is increased in PPAR $\beta/\delta$  knockout cells, suggesting that PPAR $\alpha$ , PPAR $\beta/\delta$ , and PPAR $\gamma$  compete for the same binding sites. However, relative to wild-type (WT) cells, binding of RXR is reduced in PPAR $\beta/\delta$  KO cells. This finding indicates that PPAR $\beta/\delta$  is the main factor that



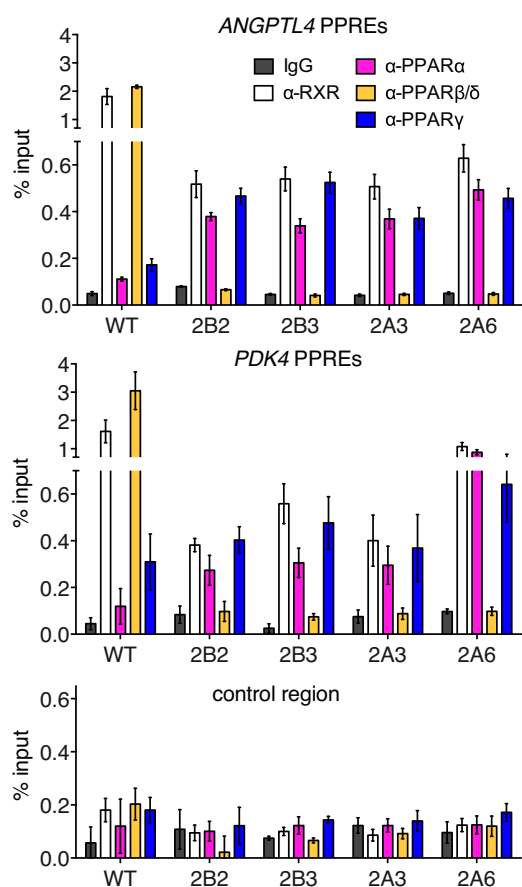


**Figure 4.** Analysis of PPAR isoform binding to chromatin in PPAR $\beta/\delta$  knockout clones. ChIP-qPCR analysis of PPAR $\alpha$ , PPAR $\beta/\delta$ , PPAR $\gamma$ , and RXR binding at the *ANGPTL4* and *PDK4* loci in the four MDA-MB231-*luc2* PPAR $\beta/\delta$  knockout clones (2B2, 2B3, 2A3, and 2A6). Parental cells (WT) were processed in parallel. A representative experiment is shown. The error bars denote standard deviations from three technical replicates.

binds to the PPREs of the *ANGPTL4* and *PDK4* genes in MDA-MB231-*luc2*. Consistently, both induction of the *ANGPTL4* transcript by the synthetic agonist L165,041 and repression by the inverse agonist PT-S264 were disrupted in the knockout clones (Supplementary Figure S6). In contrast, the PPAR $\gamma$  agonist pioglitazone retained its function and stimulated *ANGPTL4* expression. Surprisingly (for unknown reasons), the PPAR $\alpha$  agonist Wy-14643 did not induce expression of the *ANGPTL4* gene in the KO clones (Supplementary Figure S6).

#### Functional reconstitution of PPAR $\beta/\delta$ in knockout cells

In contrast to other PPAR $\beta/\delta$  knockout clones we obtained, the 2B3 clone neither showed growth defects, nor poor viability (observed in the 2A6 clone after several passages, data not shown), nor stable integration of the Cas9 expression vector (2B2, Supplementary Figure S5E) or of the transiently transfected blasticidin resistance marker (2A3; Supplementary Figure S5F). We therefore used the 2B3 clone for rescue experiments with expression vectors that encode for WT PPAR $\beta/\delta$ . Sequencing of cloned PCR fragments indicates that guide RNAs 1 and 3 result in

single-base deletions (no. 1) or insertions (no. 3; sequences from clone 2B3 are shown in Supplementary Figure S5G). In line with previous observations (53), ectopic expression of PPAR $\beta/\delta$  driven by the strong cytomegalovirus promoter led to formation of intracellular aggregates and failed to restore ligand function (data not shown). We stably transfected the 2B3 clone with a vector encoding the murine ecotropic retroviral receptor (42), allowing for ecotropic retroviral infection. The resulting 2B3-ecoR cells were then transduced with pMSCV vectors to express WT or mutant PPAR $\beta/\delta$ , driven by the comparably weak viral long terminal repeats. Expression of the mutants was confirmed on protein level (Supplementary Figure S7). We assume that PPAR $\beta/\delta$  is weakly expressed in all cellular models we analysed due to low signals on both RNA and protein levels. The level of PPAR $\beta/\delta$  ectopically expressed from pMSCV was above that of WT cells (Supplementary Figure S7). Nevertheless, both the activation and repression functions of PPAR $\beta/\delta$  were restored, albeit to lesser extent than that observed in WT cells (Supplementary Figure S8).

#### A reconstitution screen identifies PPAR $\beta/\delta$ mutants deficient in ligand response and basal repression

Using PPAR $\beta/\delta$  knockout cells, it is possible to screen for mutants which are compromised in their repressive function. We generated a panel of 80 mutants that encode for truncated proteins or proteins with one or more substitutions of amino acid residues. We preferentially mutated residues at the surface of the LBD (ligand binding domain) since the LBD is involved in NCOR interactions (54–56), and the affinity of corepressor-derived peptides to the PPAR $\beta/\delta$  LBD is enhanced by inverse agonists (5). Published X-ray crystallography structural data of the PPAR $\beta/\delta$  LBD bound to an agonist (PDB ID: 3TKM (57)), the PPAR $\alpha$  LBD bound to an inverse agonist (PDB ID: 1KKQ (55)), and the PPAR $\gamma$ -RXR heterodimer (PDB ID: 3DZY (58)) were used as reference for choosing candidate residues. The panel also includes a negative control, C91A-E92A, a double mutant of residues critical for DNA binding (59). This mutant should be defective in all functions of DNA-bound PPAR $\beta/\delta$  (basal repression, induction by agonist, repression by inverse agonist). We then performed a functional screen, intending to identify residues of PPAR $\beta/\delta$  which are necessary for basal and PT-S264-regulated repression of the *ANGPTL4* gene—mutations with functional consequences for either mode of repression should correspond to changes in NCOR binding if the effects are mediated by NCOR recruitment.

*ANGPTL4* expression was monitored by RT-qPCR in the absence (after treatment with the solvent) or the presence of a ligand. As ligands, we used either the inverse agonist PT-S264 or the agonist L165,041. Importantly, the ligands did not modulate *ANGPTL4* expression in PPAR $\beta/\delta$  knockout cells transduced with the empty vector or the DNA binding-deficient PPAR $\beta/\delta$  C91A-E92A mutant (Supplementary Figure S9 and Figure 5B). An extended description of the screen is available in the Supplementary Material including expression data for all mutants (Supplementary Appendices A–D) and a simplified

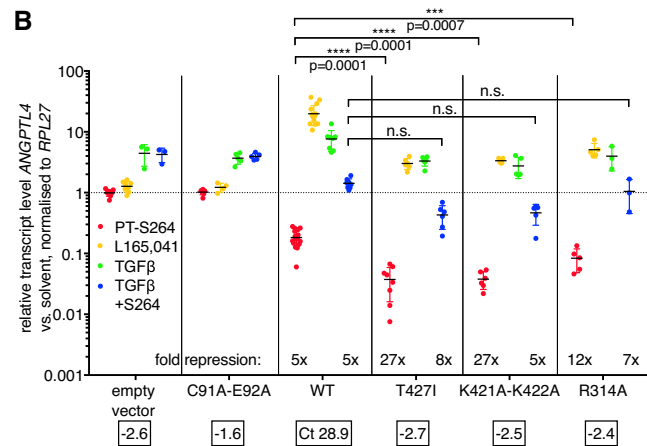
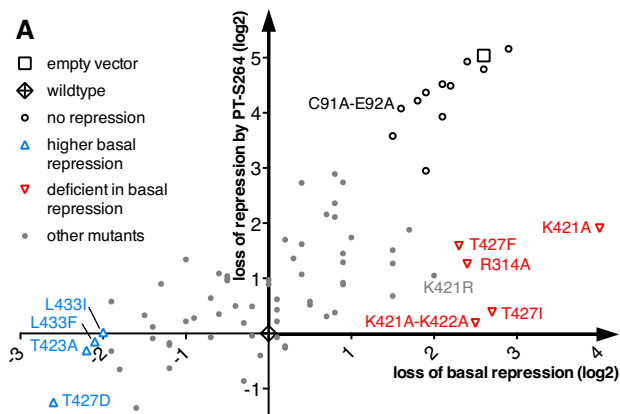


**Figure 5.** A retroviral reconstitution screen identifies PPAR $\beta/\delta$  mutants deficient in basal repression and response to PT-S264. MDA-MB231-*luc2* 2B3 PPAR KO cells stably expressing the murine ectopic receptor were transduced with retroviruses derived from the empty vector or carrying PPAR cDNAs. The WT cDNA and a panel of 80 mutants ( $N$  between 1 and 8 per construct) were used. *ANGPTL4* expression was measured by RT-qPCR after treatment for 6 h. Values were normalized to the *RPL27* transcript. (A) Effects on basal repression and PT-S264-dependent repression. *ANGPTL4* expression was plotted on the  $x$ -axis as  $\Delta\Delta$  Ct(basal WT–basal mutant) versus  $\Delta\Delta$  Ct(PT-S264 WT–PT-S264 mutant) on the  $y$ -axis. Open triangles denote mutants with modified basal repression (arbitrary cutoff of two PCR cycles relative to WT). Mean Ct values relative to the Ct value obtained from cells expressing the WT PPAR cDNA ( $N = 20$ , mean Ct 28.9) were used. (B) The relative expression of *ANGPTL4* was measured in cells transduced with the empty vector ( $N \geq 3$ ), a retrovirus carrying the C91A-E92A DNA binding mutant PPAR cDNA ( $N \geq 4$ ), the WT ( $N \geq 8$ ), the T427I ( $N \geq 6$ ), the K421A-K422A ( $N \geq 5$ ) or the R314A mutant ( $N \geq 3$ ) cDNAs and treated as indicated. The fold change relative to the solvent control sample was plotted. Significance levels were calculated via unpaired  $t$ -tests between the fold repression values.

overview with a classification of the effect of each mutant (Supplementary Table S3).

Briefly, our efforts identified several mutants which are generally compromised for receptor function, mutants which are compromised for ligand binding, mutants which show enhanced basal repression, and mutants which are deficient in basal repression. In this study, special interest pertains to mutants which affect repression. For visualization of effects on repression, we plotted the ratio of basal *ANGPTL4* expression on the  $x$ -axis as  $\Delta\Delta$  Ct(basal WT–basal mutant); the  $\Delta\Delta$  Ct term is due to the use of “ $\Delta$  Ct” values normalized to the housekeeping transcript. This way, loss of repression is reflected in a positive value.  $\Delta\Delta$  Ct(PT-S264 WT–PT-S264 mutant) is plotted on the  $y$ -axis. The reconstituted WT receptor is at (0;0), and mutations which compromise both modes of repression cluster with the empty vector control in the upper right area of the graph (Figure 5A).

Mutants modified only in basal repression cluster on or below the  $x$ -axis (Figure 5A), whereas mutants with differential capability for PT-S264-dependent repression should cluster on the  $y$ -axis. We identified both kinds of mutants; however, deficiency in PT-S264-dependent repression was accompanied by loss of response to L165,041 in the few mutants we identified, indicating that the effect is not specific for the inverse agonist since ligand binding is compromised (see Supplementary Figure S9).

Strikingly, mutants with deficient basal repression (R314A, K421A-K422A, K421A, T427F, and T427I) show enhanced repression in the presence of PT-S264. These do not markedly deviate from the  $x$ -axis (Figure 5), indicating that, while basal repression is compromised, PT-S264 is able to repress *ANGPTL4* expression to similar levels as achieved in the presence of the WT receptor (see also

Supplementary Figure S9). This implies that the observed fold repression is higher by the amount lost from basal repression (see below).

Conversely, in cells expressing mutants with enhanced basal repression (negative on the  $x$ -axis; I327A, T423A, T427D, and L433F), little or no PT-S264-stimulated repression was measured (Supplementary Figure S9). Therefore, the mutations affecting basal repression we identified here as well as the inverse agonist itself presumably modulate the affinity of PPAR $\beta/\delta$  towards the same repressors. We however cannot rule out that mutants with enhanced basal repression recruit additional other repressors. Moreover, due to low *ANGPTL4* expression levels in cells expressing these mutants, we are running into detection problems.

In the following experiments, we focus on three mutants with deficient basal repression, K421-K422A, T427I, and R314A. In Figure 5B, detailed *ANGPTL4* RT-qPCR data for these three mutants are shown. Basal repression of *ANGPTL4* is relieved in cells expressing these mutants, resulting in a higher fold repression in the presence of PT-S264, while fold induction by the agonist L165,041 is lowered. In the presence of the activating stimulus TGF $\beta$ , repression by PT-S264 is functional in cells expressing these mutants, albeit to an extent similar to cells transduced with WT PPAR $\beta/\delta$ .

The main finding of the functional screen is that loss of basal repression is fully compensated for by the inverse agonist PT-S264, resulting in higher fold repression. *Vice versa*, enhanced basal repression limits repression by PT-S264. This leads to the hypothesis that the same corepressor(s) mediate both basal and inverse agonist-dependent repression. The K421A-K422A, T427I, and R314A mutants chosen for further analysis predominantly show PT-S264-mediated repression and thus allow to investigate whether

basal repression and PT-S264-dependent repression indeed depend on the same corepressor(s). Due to data obtained by mass spectrometry (Table 1), we assume that repression is mediated by NCOR or both NCOR and SMRT.

### PPAR $\beta/\delta$ mutants deficient in basal repression show diminished NCOR and SMRT recruitment to chromatin and increased RNA polymerase II recruitment in the basal state

We next asked if the mutants deficient in basal repression indeed show differential binding of NCOR and SMRT as predicted. To this end, we analysed a panel of four PPAR $\beta/\delta$  target genes at the chromatin level. Our previous genome-wide studies identified PPAR $\beta/\delta$  binding sites and target genes in different cellular model systems (1,2,12,15) including the MDA-MB231-*luc2* cell line used here (15). The genes strongly regulated by PPAR $\beta/\delta$  ligands in cell lines are *ANGPTL4*, *PDK4*, *ABCA1*, and *PLIN2*. ChIP-qPCR analyses reveal that binding of both NCOR and SMRT to PPAR $\beta/\delta$ -responsive elements of the genes *ANGPTL4*, *PDK4*, and *PLIN2* is markedly reduced in cells that express the T427I, K421A-K422A, and R314A mutants (Figure 6). However, in the presence of PT-S264, NCOR and SMRT binding is restored by the T427I, K421A-K422A, and R314A mutants. Essentially, the same observation was made for HDAC3 (Supplementary Figure S10). As an additional control, the presence of mutated PPAR $\beta/\delta$  and RXR as well as NCOR recruitment by PT-S264 at the *ANGPTL4* PPAR binding site was confirmed (Supplementary Figure S11). Moreover, in the absence of ligand, binding of RNAPII to the *ANGPTL4*, *PDK4*, *PLIN2*, and *ABCA1* target gene TSSs is strongly reduced in *PPARD* KO cells reconstituted with WT PPAR $\beta/\delta$  (Figure 7A–D) but not in cells expressing the T427I or K421A-K422A mutants. Strikingly, PT-S264 treatment leads to reduced RNAPII binding in cells expressing these mutants. Notably, the mode of ligand binding is not altered in the mutants since an additional mutation that occludes the ligand binding pocket abrogates ligand function (see Supplementary Figure S12). RNAPII binding at the TSS of *TSC22D3*, which is not a PPAR target gene, is neither affected by expression of the PPAR $\beta/\delta$ -encoding cDNAs nor by PT-S264 (Figure 7F). This finding shows that the PPAR $\beta/\delta$  mutants deficient in basal NCOR, SMRT, and HDAC3 binding allow for increased RNAPII occupancy in the absence of activating ligands. Conversely, these mutants recruit NCOR, SMRT, and HDAC3 in the presence of the inverse agonist PT-S264, and thus RNAPII binding is strongly reduced. These observations indicate that NCOR and SMRT mediate both basal and PT-S264-dependent repression by limiting RNAPII binding to PPAR $\beta/\delta$  target genes. Strong reduction of RNAPII binding in cells expressing the T427I or K421A-K422A mutants upon short (30 min) treatment with PT-S264 strongly suggests that PPAR target genes other than *ANGPTL4*—*PDK4*, *PLIN2*, and *ABCA1* are shown here—are also regulated at the level of initiation by PT-S264. We were however unable to reliably detect GTFs and Mediator subunits at these genes, which presumably is due to their comparably low expression (see Supplementary Figure S4 for *ANGPTL4* in MDA-MB231-*luc2*) and limited sensitivity of the antibodies.

Additionally, we used samples obtained by treatment of Caki-1 cells with the initiation inhibitor triptolide and subjected to RNAPII ChIP (see Figure 1) to test whether PT-S264 mimicked the effect. Supplementary Figure S14 shows that RNAPII occupancy at the *PLIN2* TSS is reduced even more strongly than at the *ANGPTL4* TSS by PT-S264, while the effect is less pronounced at the *ABCA1* TSS; the effect of triptolide is similar but stronger. Collectively, these results implicate that PT-S264 reduces RNAPII recruitment at PPAR target genes.

### The role of deacetylase activity in repression by PT-S264

In order to investigate the role of the HDAC3 subunit of NCOR and SMRT complexes in repression of PPAR $\beta/\delta$  target genes, we treated cells with PT-S264 together with HDAC inhibitors. In WT MDA-MB231-*luc2*, neither TSA nor the HDAC3-selective compound apicidin abrogates repression of *ANGPTL4* elicited by PT-S264 (Figure 8A, upper left panel). However, repression of *ANGPTL4* is diminished by the HDAC inhibitors. PT-S264-mediated repression of *PDK4*, which is weaker in comparison to *ANGPTL4*, is also diminished by the HDAC inhibitors (Figure 8A, upper right panel), albeit to a lesser extent. Another PPAR $\beta/\delta$  target gene transcript, *PLIN2*, shows the same pattern (Figure 8A, lower left panel).

In KO cells with restored WT PPAR $\beta/\delta$  expression, PT-S264-mediated repression of *ANGPTL4* is insensitive to the HDAC inhibitors, whereas in *PPARD* KO cells expressing mutants deficient in basal repression, repression of *ANGPTL4* by PT-S264 is partially sensitive to HDAC inhibition (Figure 8B). The *PDK4* transcript is affected similarly. This clearly suggests that the NCOR and SMRT complexes recruited to PPAR $\beta/\delta$  target genes exert both deacetylase-dependent and deacetylase-independent repressive functions; the catalytic activity of HDAC3 contributes to but is not sufficient for full repression. This is in agreement with the observation that *ANGPTL4* expression is only weakly induced by HDAC inhibitors (Figure 8B and (15)).

In general, weaker repression in 2B3 cells reconstituted with the WT *PPARD* cDNA relative to the parental cells was observed (Supplementary Figure S6). We attribute this to sequestration of corepressors by overexpressed WT PPAR $\beta/\delta$ , which recruits NCOR and SMRT considerably stronger than the mutants deficient in basal repression (Figure 6). Sequestration might differentially affect the availability of free NCOR and SMRT.

## DISCUSSION

NCOR and SMRT figure in gene regulation by a multitude of transcription factors such as the glucocorticoid receptor (60,61), other nuclear receptors (6,62), POZ-containing, basic helix-loop-helix and basic leucine zipper factors (63), the Notch effector RBP-J (64), and MECP2 (methylated CpG binding protein 2) (65). Therefore, elucidation of regulatory mechanisms used by NCOR and SMRT complexes is of great interest. We show here that PPAR $\beta/\delta$  inverse agonists interfere with recruitment of the transcription-permissive Mediator subunits MED1, MED13L, and MED26 as

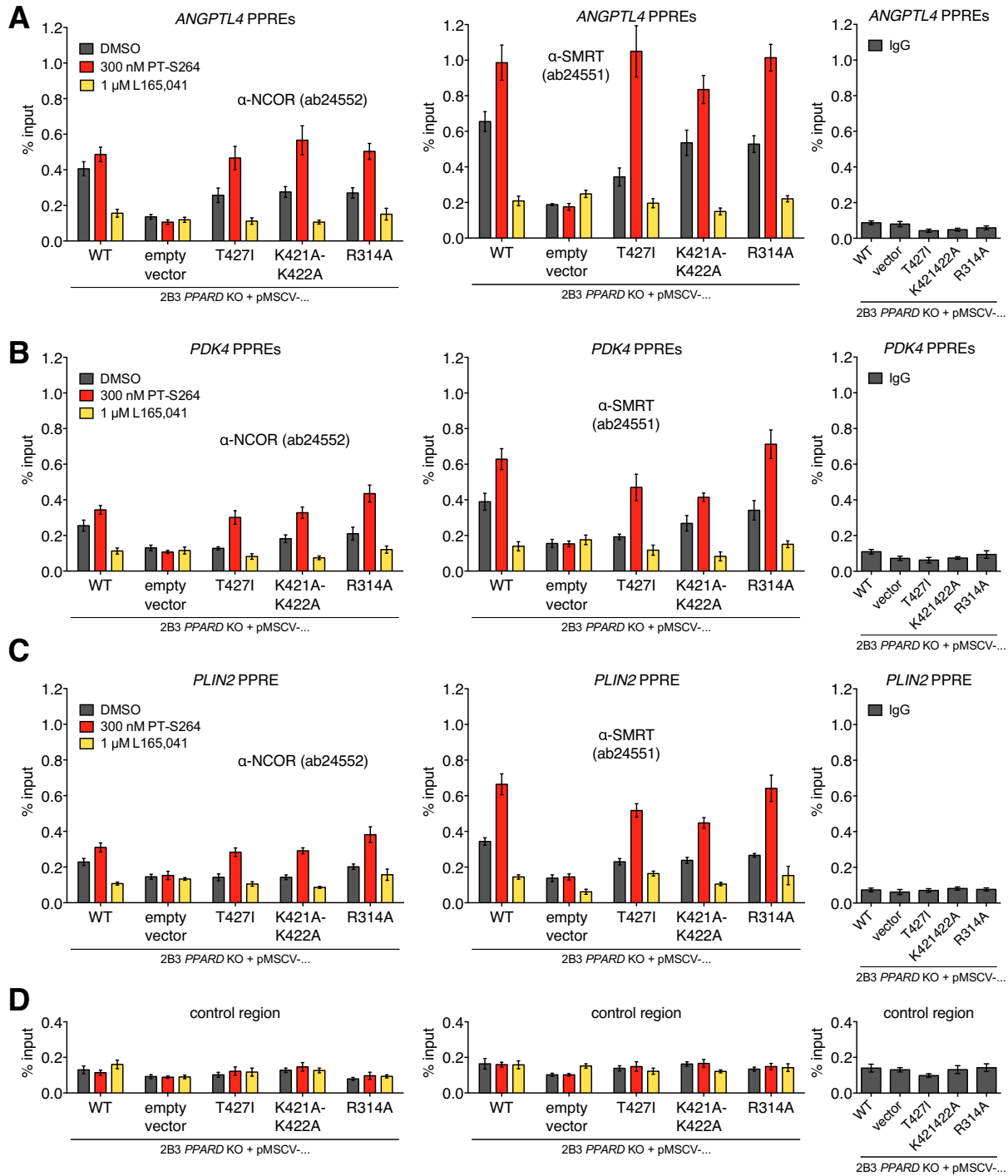


**Figure 6.** Corepressor recruitment by *PPAR* $\beta/\delta$  mutants deficient in basal repression. 2B3 *PPAR* KO cells transduced with the indicated constructs were treated with solvent, 1  $\mu$ M L165,041 or 300 nM PT-S264 for 30 min and subjected to ChIP-qPCR analysis using antibodies against NCOR or SMRT. The *PPAR* binding sites of *ANGPTL4* (+3500 bp relative to the TSS, (A), *PDK4* (-12 200 bp, (B), *PLIN2* (-34 300 bp, (C), and a negative control region (D) were amplified as indicated. Non-cognate IPs (IgG) were processed in parallel from the solvent-treated cells. Means and standard deviations of three technical replicates from a representative ChIP assay are plotted.

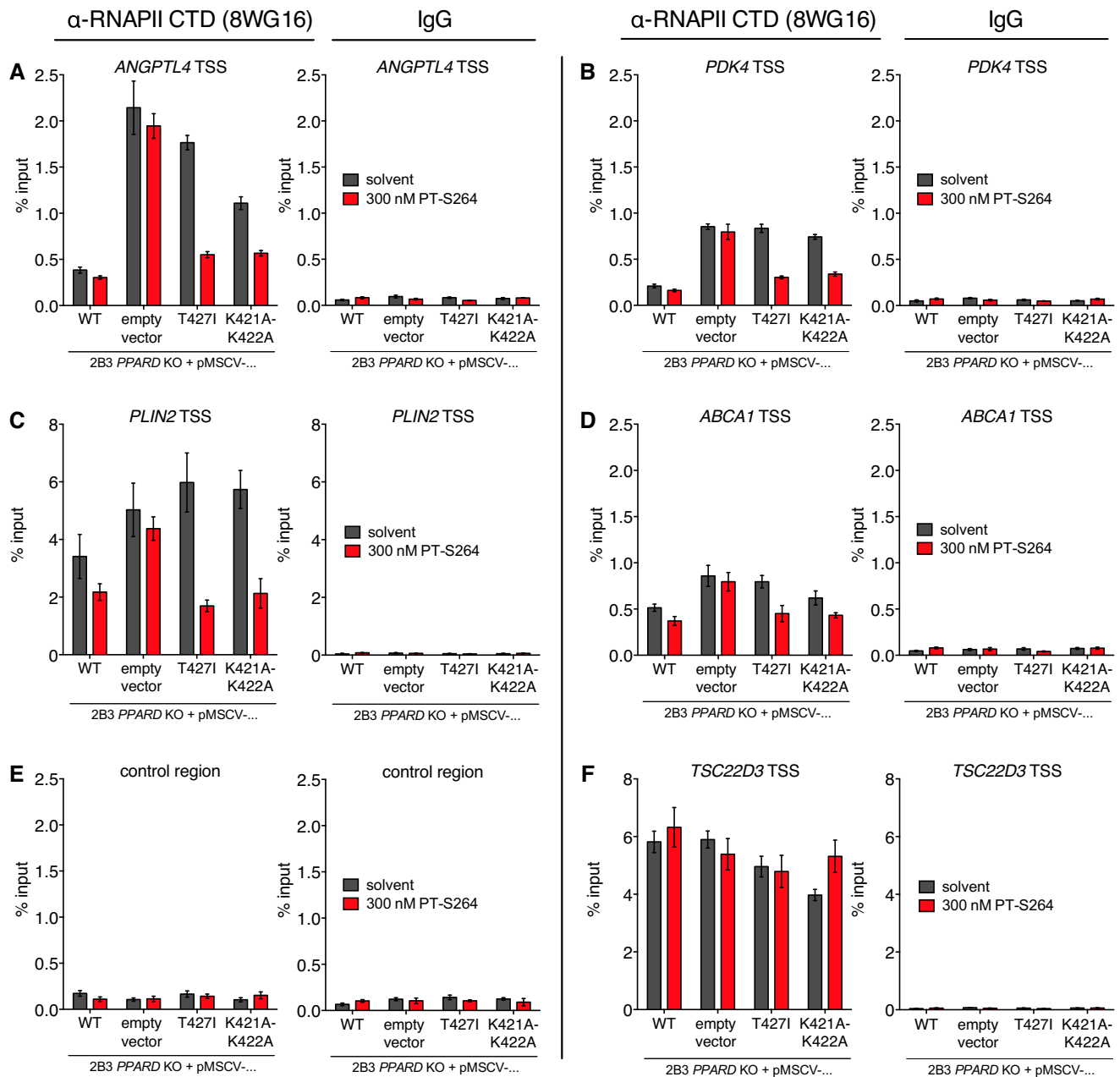


**Figure 7.** Regulation of RNA polymerase II binding by PPAR $\beta/\delta$  mutants deficient in basal repression. 2B3 PPAR KO cells transduced with the indicated constructs were treated with solvent or 300 nM PT-S264 for 30 min and subjected to ChIP-qPCR analysis using an antibody against RNA polymerase II. The TSS regions of *ANGPTL4* (A), *PDK4* (B), *PLIN2* (C), *ABCA1* (D), a negative control region (E), and the *TSC22D3* TSS (F) as an additional negative control were amplified as indicated. Means and standard deviations of three technical replicates from a representative ChIP assay are plotted.

well as TFIIB and RNAPII. PPAR $\beta/\delta$  mutants deficient in NCOR and SMRT recruitment in the basal state allow for enhanced RNAPII binding in the absence of ligands, while the inverse agonist PT-S264 restores both NCOR and SMRT binding to these mutants and loss of RNAPII at target gene promoters. Repression is only partially sensitive to HDAC inhibition, which indicates that NCOR/SMRT complexes exert deacetylase-dependent and deacetylase-independent functions to restrain transcription of PPAR $\beta/\delta$  target genes.

HDAC-independent repression mechanisms exerted by NCOR/SMRT have also been reported in other contexts: (i) In mice, Ncor and Smrt complexes carry out essential functions that are independent of Hdac3 activity (66), and (ii) HDAC-independent repression of human papillomavirus transcription and replication by NCOR was demonstrated (67). (iii) Finally, whereas MECP2 represses transcription via an HDAC-independent mechanism (68), interaction with NCOR/SMRT is crucial for MECP2 function (65), and it was reported recently that the detrimental

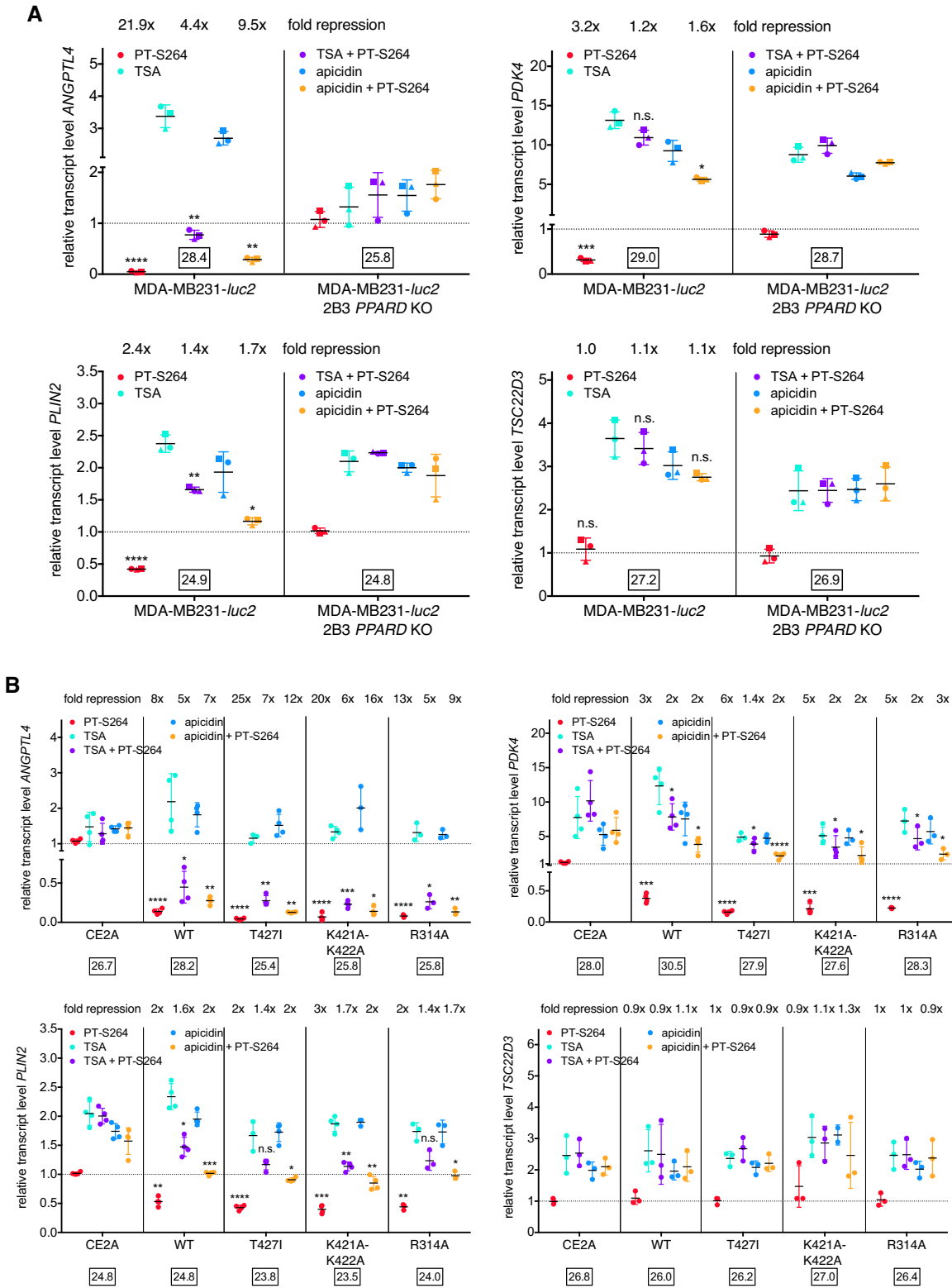


**Figure 8.** HDAC inhibitor sensitivity of PT-S264-mediated repression. Parental MDA-MB231-*luc2* and 2B3 *PPARD* KO cells (A) or 2B3 *PPARD* KO cells transduced with the indicated constructs (B) were treated with solvent, 300 nM PT-S264, 500 nM TSA, and 250 nM apicidin as indicated for 6 h, and RT-qPCR with primers against the *ANGPTL4*, *PDK4*, *PLIN2*, and *TSC22D3* transcripts was performed. Means and standard deviations of (A)  $n = 3$  independent experiments or (B)  $n = 3-4$  independent experiments are plotted. Mean normalized Ct values in the control condition are indicated. Significance levels were calculated via paired *t*-tests. \*\*\*\*,  $P < 0.0001$ ; \*\*\*,  $P < 0.001$ ; \*\*,  $P < 0.01$ ; \*,  $P < 0.05$ ; n.s., not significant.

effects of Mecp2 overexpression in mice do not depend on the catalytic activity of Hdac3 (69).

Our data suggest that deacetylation by HDAC3 contributes to but is not sufficient for basal repression of PPAR $\beta/\delta$  target genes. Thus, an additional enzymatic function of HDAC3-containing complexes or, alternatively, inhibition of an activator-borne enzymatic activity may be required for efficient silencing of gene expression. We speculate that acetyltransferases are inhibited by NCOR and SMRT complexes since (i) acetyltransferase activity is required for transcription in nucleosome-free systems (70), (ii) GTFs that contribute to reinitiation—TFIIB, TFIIE, and TFIIIF—are acetylated *in vivo* (71,72), and (iii) the acetyltransferase activities of CBP and p300 are inhibited by recombinant purified fragments of NCOR and SMRT *in vitro* (73,74). Moreover, Mediator interacts with the acetyltransferase-bearing SAGA complex, and both Mediator and SAGA are necessary for RNAPII-mediated transcription in yeast (75–77). Partial sensitivity of PT-S264-dependent repression to HDAC inhibitors (Figure 8) strongly suggests that NCOR and SMRT recruited by PPAR $\beta/\delta$  use an additional mechanism to restrict activator function. It is striking that, in cells ectopically expressing PPAR $\beta/\delta$  mutants with deficient basal repression, PT-S264-dependent repression is more sensitive to HDAC inhibition than in cells ectopically expressing the WT receptor (Figure 8B). This finding suggests that the NCOR/SMRT complexes involved in basal repression, whose binding is restored by PT-S264 in cells expressing the mutants (Figure 6), rely on HDAC activity to a larger extent compared to the complexes that are recruited to the WT receptor upon treatment with PT-S264.

Induction of the PPAR $\beta/\delta$  target gene *ANGPTL4* by TGF $\beta$  depends on SMAD3 (18), which interacts with CBP and p300 to activate transcription (78). CBP and p300 are also paramount coactivators of NF $\kappa$ B (79) and AP-1 (80) transcription factors, which are major targets of transrepression by nuclear receptors (61,80–82). These data underscore a possible role for acetyltransferase inhibition in gene regulation by NCOR and SMRT. Since deacetylation and inhibition of acetyltransferase activity act towards the same outcome, the two functions may conceivably act in parallel for more efficient suppression of transcription. Another possibility would be that ubiquitin ligase and deubiquitinase activities which reside in subunits of HDAC3-containing complexes contribute to deacetylase-independent repression. Ubiquitination by TBLR1 (6) could commit activators for degradation, or H2B deubiquitination by USP44 might figure in repression of *ANGPTL4* by NCOR/SMRT (36).

Mediator supports TFIIB binding to promoters, and both Mediator and TFIIB facilitate recruitment of RNAPII to promoter-bound GTFs (30). This notion is in agreement with both older and more recent studies in yeast (47,75,83,84), murine (85), and human cells (86) which indicate concurrent interactions of Mediator, TFIIB, and RNAPII. MS data from *S. cerevisiae* and from human cells identify RNAPII, TFIIB, and TFIIIF amongst the strongest interactors of Mediator (75,86), and these factors are necessary for reinitiation (25). Notably, another recent study revealed that human genes which require *de novo* RNAPII

recruitment for induction of transcription depend on TFIIB availability (87). It is unclear how transcription factors modulate reinitiation, and *in vivo* evidence of reinitiation and scaffold complexes is lacking (32). Our ChIP data (Figure 1 and Supplementary Figure S2), which demonstrate impairment of TFIIB and RNAPII binding by PPAR $\beta/\delta$  inverse agonists, are in agreement with findings obtained from *in vitro* systems that describe recruitment of RNAPII and TFIIB (25,30) to scaffold factors and thus may represent *in vivo* correlates of reinitiation and scaffold complexes. RNAPII binding to the *ANGPTL4* promoter is affected similarly by PT-S264 and the TFIIB-XPB inhibitor (88) triptolide (Figure 1A); triptolide is expected to affect both initiation and reinitiation. Our ChIP data do not allow for discrimination between the first and subsequent rounds of transcription; hence, we cannot conclude whether the first round of transcription is affected as well.

Our observations furthermore suggest that TFIIB and RNAPII recruitment coincides with the presence of MED1, MED13L, and MED26 (Figure 2). This notion is supported by previous work of others which identified MED1 (48,49), MED13L (52), and MED26 (52,89,90) as subunits that are predominantly present in RNAPII-associated Mediator. Our observations are compatible with the model that the MED13-containing kinase module blocks RNAPII association with Mediator (31) since MED26 and MED13 binding is mutually exclusive (52). Notably, co-occurrence of MED13L and MED26 was described (48,52,89,90). Our model thus favours an RNAPII-associated Mediator state which harbours the MED1, MED13L, and MED26 subunits, and this is counteracted by PT-S264 at PPAR $\beta/\delta$  target genes.

It should be noted that we cannot formally exclude involvement of corepressors other than NCOR and SMRT in PT-S264-dependent repression. Genetic deletion of *NCOR1* was unsuccessful in our hands; this is consistent with the notions that NCOR function may be necessary for regulation of the cell cycle (91), genome stability (92), or other critical processes (62). Cellular models without this limitation or knock-in approaches might be suitable to resolve whether NCOR and SMRT complexes are sufficient for repression by PPAR $\beta/\delta$  inverse agonists. Modification of endogenous coding sequences would also circumvent possible effects of overexpression such as cofactor sequestration. Notably, after reconstitution of PPAR $\beta/\delta$  expression, PT-S264-dependent repression is largely insensitive to HDAC inhibition, which is in contrast to partial sensitivity observed in the parental cell line. Moreover, HDAC inhibition leads to weaker upregulation of PPAR $\beta/\delta$  target genes in the parental cells compared to cells with reconstituted PPAR $\beta/\delta$ . This could be due to higher recruitment of SMRT relative to recruitment of NCOR after reconstitution of PPAR $\beta/\delta$  expression (Figure 6), whereas the ratio of ChIP-qPCR signals obtained with the same antibodies is closer to one in WT cells (Figure 3). However, the preferential dependence of SMRT complexes on deacetylase activity relative to NCOR complexes is highly speculative.

Taken together, we propose that PPAR $\beta/\delta$  recruits NCOR and SMRT, either of which or both block MED1, MED13L, and MED26 recruitment to promoter-bound GTFs via both deacetylase-dependent and -independent

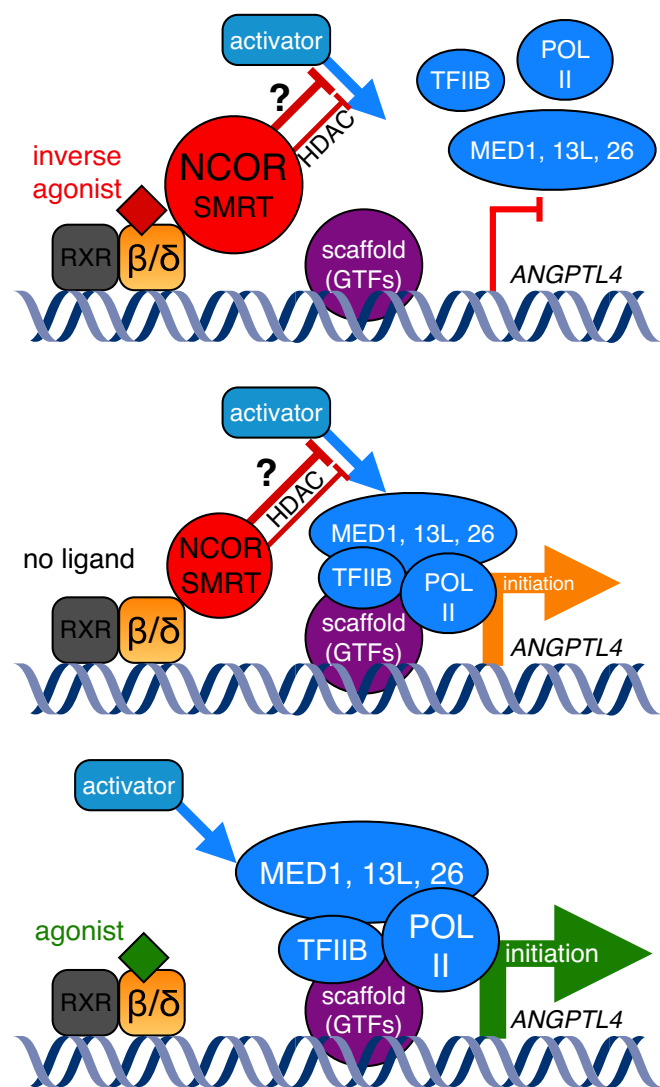


**Figure 9.** Ligand-dependent regulation of *ANGPTL4* transcription initiation by PPAR $\beta/\delta$  and NCOR/SMRT. Data from this study show that the PPAR $\beta/\delta$  inverse agonist PT-S264 interferes with activator-stimulated recruitment of MED1, MED13L, MED26, TFIIB, and RNAPII. Mutations of PPAR $\beta/\delta$  which abrogate NCOR and SMRT binding in the basal state allow for increased binding of RNAPII, and NCOR and SMRT binding is restored upon addition of PT-S264. The latter observations were made at other PPAR target genes as well. Taken together with our previous observation that synthetic PPAR agonists together with other activating stimuli synergistically induce *ANGPTL4* transcription (18), we propose the model that basal and ligand-dependent repressor recruitment limit the ability of activators to induce transcription reinitiation (and possibly initiation) via NCOR, SMRT, or both. The corepressors use both deacetylase-dependent and deacetylase-independent mechanisms, the latter of which are not elucidated as of now.

functions to interfere with TFIIB and RNAPII binding. A model depicted in Figure 9 summarizes our conclusions. Additional insight will require identification of the subunits and domains of NCOR and SMRT complexes which exert deacetylase-independent repression and their target proteins, and it will be interesting to probe possible differential functions of NCOR and SMRT.

## DATA AVAILABILITY

The mass spectrometry proteomics data have been deposited to the ProteomeXchange Consortium via the PRIDE (93) partner repository with the dataset identifier PXD012818 and 10.6019/PXD012818.

## SUPPLEMENTARY DATA

Supplementary Data are available at NAR Online.

## ACKNOWLEDGEMENTS

We gratefully acknowledge the performance of RIME assays by Garrett Shafer (Active Motif, Inc.) and the help of Matthias Spiller-Becker (Active Motif, Inc.), Tiffany Yen (Active Motif, Inc.), and Florian Finkernagel with mass spectrometry data. We thank Guntram Suske, Ho-Ryun Chung, Nathalie Hoffmann, and Florian Finkernagel for helpful discussions and critical reading of the manuscript. *Authors' contributions:* Conceived, designed, and performed the experiments: N.L. and T.A.; N.L. performed the vast majority of the experiments. Analysed data: N.L., B.F., and T.A. Generated and contributed reagents and materials: N.L., C.L.B., S.Z., B.W., M.D., W.E.D., and T.A. Supervised the study and wrote the paper: T.A.

## FUNDING

Deutsche Forschungsgemeinschaft [AD474/1-1 to T.A., DI827/4-1 to W.E.D.]. Funding for open access charge: Deutsche Forschungsgemeinschaft [AD474/1-1 to T.A.]; Philipps University of Marburg, Department of Medicine.

*Conflict of interest statement.* None declared.

## REFERENCES

- Adhikary, T., Kaddatz, K., Finkernagel, F., Schönbauer, A., Meissner, W., Scharfe, M., Jarek, M., Blöcker, H., Müller-Brüsselbach, S. and Müller, R. (2011) Genomewide analyses define different modes of transcriptional regulation by peroxisome proliferator-activated receptor- $\beta/\delta$  (PPAR $\beta/\delta$ ). *PLoS One*, **6**, e16344.
- Adhikary, T., Wortmann, A., Schumann, T., Finkernagel, F., Lieber, S., Roth, K., Toth, P.M., Diederich, W.E., Nist, A., Stiewe, T. *et al.* (2015) The transcriptional PPAR $\beta/\delta$  network in human macrophages defines a unique agonist-induced activation state. *Nucleic Acids Res.*, **43**, 5033–5051.
- Shi, Y., Hon, M. and Evans, R.M. (2002) The peroxisome proliferator-activated receptor  $\delta$ , an integrator of transcriptional repression and nuclear receptor signaling. *Proc. Natl. Acad. Sci. U.S.A.*, **99**, 2613–2618.
- Krogdram, A.M., Nielsen, C.A.F., Neve, S., Holst, D., Helledie, T., Thomsen, B., Bendixen, C., Mandrup, S. and Kristiansen, K. (2002) Nuclear receptor corepressor-dependent repression of peroxisome-proliferator-activated receptor  $\delta$ -mediated transactivation. *Biochem. J.*, **363**, 157–165.
- Naruh, S., Toth, P.M., Adhikary, T., Kaddatz, K., Pape, V., Dörr, S., Klebe, G., Müller-Brüsselbach, S., Diederich, W.E. and Müller, R. (2011) High-affinity peroxisome proliferator-activated receptor  $\beta/\delta$ -specific ligands with pure antagonistic or inverse agonistic properties. *Mol. Pharmacol.*, **80**, 828–838.
- Mottis, A., Mouchiroud, L. and Auwerx, J. (2013) Emerging roles of the corepressors NCoR1 and SMRT in homeostasis. *Genes Dev.*, **27**, 819–835.



7. Oberoi, J., Fairall, L., Watson, P.J., Yang, J.C., Czimmerer, Z., Kampmann, T., Goult, B.T., Greenwood, J.A., Gooch, J.T., Kallenberger, B.C. *et al.* (2011) Structural basis for the assembly of the SMRT/NCOR core transcriptional repression machinery. *Nat. Struct. Mol. Biol.*, **18**, 177–184.
8. Guo, C., Gow, C.H., Li, Y., Gardner, A., Khan, S. and Zhang, J. (2011) Regulated clearance of histone deacetylase 3 protects independent formation of nuclear receptor corepressor complexes. *J. Biol. Chem.*, **287**, 12111–12120.
9. You, S.H., Lim, H.W., Sun, Z., Broache, M., Won, K.J. and Lazar, M.A. (2013) Nuclear receptor co-repressors are required for the histone-deacetylase activity of HDAC3 in vivo. *Nat. Struct. Mol. Biol.*, **20**, 182–187.
10. Forman, B.M., Chen, Y. and Evans, R.M. (1997) Hypolipidemic drugs, polyunsaturated fatty acids, and eicosanoids are ligands for peroxisome proliferator-activated receptors  $\alpha$  and  $\delta$ . *Proc. Natl. Acad. Sci. U.S.A.*, **94**, 4312–4317.
11. Naruhn, S., Meissner, W., Adhikary, T., Kaddatz, K., Klein, T., Watzel, B., Müller-Brüsselbach, S. and Müller, R. (2010) 15-hydroxyeicosatetraenoic acid is a preferential peroxisome proliferator-activated receptor  $\beta/\delta$  agonist. *Mol. Pharmacol.*, **77**, 171–184.
12. Schumann, T., Adhikary, T., Wortmann, A., Lieber, S., Schnitzer, E., Legrand, N., Schober, Y., Nockher, A.W., Toth, P.M., Diederich, W.E. *et al.* (2015) Deregulation of PPAR $\beta/\delta$  target genes in tumor-associated macrophages by fatty acid ligands in the ovarian cancer microenvironment. *Oncotarget*, **6**, 13416–13433.
13. Klingler, C., Zhao, X., Adhikary, T., Li, J., Xu, G., Häring, H.U., Schleicher, E. and Weigert, C. (2016) Lysophosphatidylcholines activate PPAR $\delta$  and protect human skeletal muscle cells from lipotoxicity. *Biochim. Biophys. Acta*, **1861**, 1980–1992.
14. Lieber, S., Scheer, F., Meissner, W., Naruhn, S., Adhikary, T., Müller-Brüsselbach, S., Diederich, W.E. and Müller, R. (2012) (*Z*)-2-(2-Bromophenyl)-3-[4-(1-methylpiperazine)amino]phenylacrylonitrile (DG172): an orally bioavailable PPAR $\beta/\delta$ -selective ligand with inverse agonistic properties. *J. Med. Chem.*, **55**, 2858–2868.
15. Adhikary, T., Brandt, D.T., Kaddatz, K., Stockert, J., Naruhn, S., Meissner, W., Finkernagel, F., Obert, J., Lieber, S., Scharfe, M. *et al.* (2013) Inverse PPAR $\beta/\delta$  agonists suppress oncogenic signaling to the *ANGPTL4* gene and inhibit cancer cell invasion. *Oncogene*, **32**, 5241–5252.
16. Toth, P.M., Lieber, S., Scheer, F.M., Schumann, T., Schober, Y., Nockher, W.A., Adhikary, T., Müller-Brüsselbach, S., Müller, R. and Diederich, W.E. (2016) Design and synthesis of highly active Peroxisome Proliferator-Activated Receptor (PPAR)  $\beta/\delta$  inverse agonists with prolonged cellular activity. *Chemmedchem*, **11**, 488–496.
17. Zhu, P., Goh, Y., Chin, A.H.F., Kersten, S. and Tan, N.S. (2012) Angiopoietin-like 4: a decade of research. *Biosci. Rep.*, **32**, 211–219.
18. Kaddatz, K., Adhikary, T., Finkernagel, F., Meissner, W., Müller-Brüsselbach, S. and Müller, R. (2010) Transcriptional profiling identifies functional interactions of TGF $\beta$  and PPAR $\beta/\delta$  signaling: synergistic induction of *ANGPTL4* transcription. *J. Biol. Chem.*, **285**, 29469–29479.
19. Inoue, T., Kohro, T., Tanaka, T., Kanki, Y., Li, G., Poh, H.M., Mimura, I., Kobayashi, M., Taguchi, A., Maejima, T. *et al.* (2014) Cross-enhancement of *ANGPTL4* transcription by HIF1 $\alpha$  and PPAR $\beta/\delta$  is the result of the conformational proximity of two response elements. *Genome Biol.*, **15**, R63.
20. Roeder, R.G. (1996) The role of general initiation factors in transcription by RNA polymerase II. *Trends Biochem. Sci.*, **21**, 327–335.
21. Kornberg, R.D. (1998) Mechanism and regulation of yeast RNA polymerase II transcription. *Cold Spring Harb. Symp. Quant. Biol.*, **63**, 229–232.
22. Conaway, R.C., Sato, S., Tomomori-Sato, C., Yao, T. and Conaway, J.W. (2005) The mammalian Mediator complex and its role in transcriptional regulation. *Trends Biochem. Sci.*, **30**, 250–255.
23. Kornberg, R.D. (2005) Mediator and the mechanism of transcriptional activation. *Trends Biochem. Sci.*, **30**, 250–255.
24. Malik, S. and Roeder, R.G. (2005) Dynamic regulation of pol II transcription by the mammalian Mediator complex. *Trends Biochem. Sci.*, **30**, 256–263.
25. Yudkovsky, N., Ranish, J.A. and Hahn, S. (2000) A transcription reinitiation intermediate that is stabilized by activator. *Nature*, **408**, 225–229.
26. Shandilya, J. and Roberts, S.G.E. (2012) The transcription cycle in eukaryotes: from productive initiation to RNA polymerase II recycling. *Biochim. Biophys. Acta*, **1819**, 391–400.
27. Singh, B.N. and Hampsey, M. (2007) A transcription-independent role for TFIIB in gene looping. *Mol. Cell*, **27**, 806–816.
28. El Kaderi, B., Medler, S., Raghunayakula, S. and Ansari, A. (2009) Gene looping is conferred by activator-dependent interaction of transcription initiation and termination machineries. *J. Biol. Chem.*, **284**, 25015–25025.
29. Medler, S., Al Husini, N., Raghunayakula, S., Mukundan, B., Aldea, A. and Ansari, A. (2011) Evidence for a complex of transcription factor IIB (TFIIB) with Poly(A) polymerase and cleavage factor 1 subunits required for gene looping. *J. Biol. Chem.*, **286**, 33709–33718.
30. Baek, H.J., Kang, Y.K. and Roeder, R.G. (2006) Human mediator enhances basal transcription by facilitating recruitment of transcription factor IIB during preinitiation complex assembly. *J. Biol. Chem.*, **281**, 15172–15181.
31. Knuesel, M.T., Meyer, K.D., Bernecky, C. and Taatjes, D.J. (2009) The human CDK8 subcomplex is a molecular switch that controls Mediator coactivator function. *Genes Dev.*, **23**, 439–451.
32. Soutourina, J. (2017) Transcription regulation by the Mediator complex. *Nat. Rev. Mol. Cell Biol.*, **19**, 262–274.
33. Mandar, S., Zandbergen, F., Tan, N.S., Escher, P., Patsouris, D., Koenig, W., Kleemann, R., Bakker, A., Veenman, F., Wahli, W. *et al.* (2004) The direct peroxisome proliferator-activated receptor target fasting-induced adipose factor (FIAF/PGAR/ANGPTL4) is present in blood plasma as a truncated protein that is increased by fenofibrate treatment. *J. Biol. Chem.*, **279**, 34411–34420.
34. Staiger, H., Haas, C., Machann, J., Werner, R., Weisser, M., Schick, F., Machicao, F., Stefan, N., Fritsche, A. and Häring, H.U. (2009) Muscle-derived angiopoietin-like protein 4 is induced by fatty acids via peroxisome proliferator-activated receptor (PPAR)- $\delta$  and is of metabolic relevance in humans. *Diabetes*, **58**, 579–589.
35. Jin, Q., Yu, L.R., Wang, L., Zhang, Z., Kasper, L.H., Lee, J.E., Wang, C., Brindle, P.K., Dent, S.Y.R. and Ge, K. (2011) Distinct roles of GCN5/PCAF-mediated H3K9ac and CBP/p300-mediated H3K18/27ac in nuclear receptor transactivation. *EMBO J.*, **30**, 249–262.
36. Lan, X., Atanassov, B.S., Li, W., Zhang, Y., Florens, L., Mohan, R.D., Galardy, P.J., Washburn, M.P., Workman, J.L. and Dent, S.Y. (2016) USP44 is an integral component of N-CoR that contributes to gene repression by deubiquitinating histone H2B. *Cell Rep.*, **17**, 2382–2393.
37. Palancade, B. and Bensaude, O. (2003) Investigating RNA polymerase II carboxyl-terminal domain (CTD) phosphorylation. *Eur. J. Biochem.*, **270**, 3859–3870.
38. Hintermair, C., Heidemann, M., Koch, F., Descostes, N., Gut, M., Gut, I., Fenouil, R., Ferrier, P., Flatley, A., Kremmer, E. *et al.* (2012) Threonine-4 of mammalian RNA polymerase II CTD is targeted by Polo-like kinase 3 and required for transcriptional elongation. *EMBO J.*, **31**, 2784–2797.
39. Chapman, R.D., Heidemann, M., Albert, T.K., Mailhammer, R., Flatley, A., Meisterernst, M., Kremmer, E. and Eick, D. (2007) Transcribing RNA polymerase II is phosphorylated at CTD residue serine-7. *Science*, **318**, 1780–1782.
40. Kinsella, T.M. and Nolan, G.P. (1996) Episomal vectors rapidly and stably produce high-titer recombinant retrovirus. *Hum. Gene Ther.*, **7**, 1405–1413.
41. Voorhoeve, P.M. and Agami, R. (2003) The tumor-suppressive functions of the human *INK4A* locus. *Cancer Cell*, **4**, 311–319.
42. Serrano, M., Lin, A.W., McCurrach, M.E., Beach, D. and Lowe, S.W. (1997) Oncogenic *ras* provokes premature cell senescence associated with accumulation of p53 and p16<sup>INK4a</sup>. *Cell*, **88**, 593–602.
43. Adhikary, T. and Müller, R. (2013) In vivo studies of PPAR-chromatin interactions: chromatin immunoprecipitation for single-locus and genome-wide analyses. *Methods Mol. Biol.*, **952**, 175–185.
44. Unger, A., Finkernagel, F., Hoffmann, N., Neuhaus, F., Joos, B., Nist, A., Stiewe, T., Visekruna, A., Wagner, U., Reinartz, S. *et al.* (2018) Chromatin binding of c-REL and p65 is not limiting for macrophage *IL12B* transcription during immediate suppression by ovarian carcinoma ascites. *Front. Immunol.*, **9**, 1425.

45. Mohammed, H., D'Santos, C., Serandour, A.A., Ali, H.R., Brown, G.D., Atkins, A., Rueda, O.M., Holmes, K.A., Theodorou, V., Robinson, J.L.L. *et al.* (2013) Endogenous purification reveals GREB1 as a key estrogen receptor regulatory factor. *Cell Rep.*, **3**, 342–349.
46. Toth, P.M., Naruhn, S., Pape, V.F., Dörr, S.M., Klebe, G., Müller, R. and Diederich, W.E. (2012) Development of improved PPAR $\beta$ / $\delta$  inhibitors. *Chemmedchem*, **7**, 159–170.
47. Eychenne, T., Novikova, E., Barrault, M.B., Alibert, O., Boschiero, C., Peixeiro, N., Cornu, D., Redeker, V., Kuras, L., Nicolas, P. *et al.* (2016) Functional interplay between Mediator and TFIIB in preinitiation complex assembly in relation to promoter architecture. *Genes Dev.*, **30**, 2119–2132.
48. Mittler, G., Kremmer, E., Timmers, H.T. and Meisterernst, M. (2001) Novel critical role of a human Mediator complex for basal RNA polymerase II transcription. *EMBO Rep.*, **2**, 808–813.
49. Zhang, X., Krutchinsky, A., Fukuda, A., Chen, W., Yamamura, S., Chait, B.T. and Roeder, R.G. (2005) MED1/TRAP220 exists predominantly in a TRAP/Mediator subpopulation enriched in RNA Polymerase II and is required for ER-Mediated transcription. *Mol. Cell*, **19**, 89–100.
50. Takahashi, H., Parmely, T.J., Sato, S., Tomomori-Sato, C., Banks, C.A.S., Kong, S.E., Szutorisz, H., Swanson, S.K., Martin-Brown, S., Washburn, M.P. *et al.* (2011) Human mediator subunit MED26 functions as a docking site for transcription elongation factors. *Cell*, **146**, 92–104.
51. Jeronimo, C. and Robert, F. (2017) The mediator complex: at the nexus of RNA polymerase II transcription. *Trends Cell Biol.*, **27**, 765–783.
52. Daniels, D.L., Ford, M., Schwinn, M.K., Benink, H., Galbraith, M.D., Amunugama, R., Jones, R., Allen, D., Okazaki, N., Yamakawa, H. *et al.* (2013) Mutual exclusivity of MED12/MED12L, MED13/13L, and CDK8/19 paralogs revealed within the CDK-Mediator kinase module. *J. Proteomics Bioinform.*, **S2**, 1–7.
53. Rieck, M., Wedeken, L., Müller-Brüsselbach, S. and Müller, R. (2007) Expression level and agonist-binding affect the turnover, ubiquitination and complex formation of peroxisome proliferator activated receptor beta. *FEBS J.*, **274**, 5068–5076.
54. Perissi, V., Staszewski, L.M., McInerney, E.M., Kurokawa, R., Krones, A., Rose, D.W., Lambert, M.H., Milburn, M.V., Glass, C.K. and Rosenfeld, M.G. (1999) Molecular determinants of nuclear receptor–corepressor interaction. *Genes Dev.*, **13**, 3198–3208.
55. Xu, E.H., Stanley, T.B., Montana, V.G., Lambert, M.H., Shearer, B.G., Cobb, J.E., McKee, D.D., Galardi, C.M., Plunket, K.D., Nolte, R.T. *et al.* (2002) Structural basis for antagonist-mediated recruitment of nuclear co-repressors by PPAR $\alpha$ . *Nature*, **415**, 813–817.
56. Yu, C., Markan, K., Temple, K.A., Deplewski, D., Brady, M.J. and Cohen, R.N. (2005) NCoR and SMRT decrease peroxisome Proliferator-activated receptor  $\gamma$  transcriptional activity and repress 3T3-L1 adipogenesis. *J. Biol. Chem.*, **280**, 13600–13605.
57. Batista, F.A.H., Trivella, D.B.B., Bernardes, A., Gratieri, J., Oliveira, P.S.L., Figueira, A.C.M., Webb, P. and Poliparkarpov, I. (2012) Structural insights into human peroxisome proliferator activated receptor delta (PPAR-Delta) selective ligand binding. *PLoS One*, **7**, e33643.
58. Chandra, V., Huang, P., Hamuro, Y., Raghuram, S., Wang, Y., Burris, T.P. and Rastinejad, F. (2008) Structure of the intact PPAR- $\gamma$ -RXR- nuclear receptor complex on DNA. *Nature*, **456**, 350–356.
59. Aagaard, M.M., Siersbaek, R. and Mandrup, S. (2011) Molecular basis for gene-specific transactivation by nuclear receptors. *Biochim. Biophys. Acta*, **1812**, 824–835.
60. Hua, G., Paulen, L. and Chambon, P. (2016) GR SUMOylation and formation of an SUMO-SMRT/ NCoR1-HDAC3 repressing complex is mandatory for GC-induced IR nGRE-mediated transrepression. *Proc. Natl. Acad. Sci. U.S.A.*, **113**, E626–E634.
61. Hua, G., Ganti, K.P. and Chambon, P. (2016) Glucocorticoid-induced tethered transrepression requires SUMOylation of GR and formation of a SUMO-SMRT/NCoR1-HDAC3 repressing complex. *Proc. Natl. Acad. Sci. U.S.A.*, **113**, E635–E643.
62. Jepsen, K., Hermanson, O., Onami, T.M., Gleiberman, A.S., Lunyak, V., McEvilly, R.J., Kurokawa, R., Kumar, V., Liu, F., Seto, E. *et al.* (2000) Combinatorial roles of the nuclear receptor corepressor in transcription and development. *Cell*, **102**, 753–763.
63. Burke, L.J. and Baniahmad, A. (2000) Co-repressors 2000. *FASEB J.*, **14**, 1876–1888.
64. Oswald, F., Rodriguez, P., Giaimo, B.D., Antonello, Z.A., Mira, L., Mittler, G., Thiel, V.N., Collins, K.J., Tabaja, N., Cizelsky, W. *et al.* (2016) A phospho-dependent mechanism involving NCoR and KMT2D controls a permissive chromatin state at Notch target genes. *Nucleic Acids Res.*, **44**, 4703–4720.
65. Lyst, M.J., Ekiert, R., Ebert, D.H., Merusi, C., Nowak, J., Selfridge, J., Guy, J., Kastan, N.R., Robinson, N.D., de Lima Alves, F. *et al.* (2013) Rett syndrome mutations abolish the interaction of MeCP2 with the NCoR/SMRT co-repressor. *Nat. Neurosci.*, **16**, 898–902.
66. Sun, Z., Feng, D., Fang, B., Mullican, S.E., You, S.H., Lim, H.W., Everett, L.J., Nabel, C.S., Li, Y., Selvakumaran, V. *et al.* (2013) Deacetylase-independent function of HDAC3 in transcription and metabolism requires nuclear receptor corepressor. *Mol. Cell*, **52**, 769–782.
67. Dreer, M., Fertey, J., van de Poel, S., Straub, E., Madlung, J., Macek, B., Iftner, T. and Stubenrauch, F. (2016) Interaction of NCOR/SMRT repressor complexes with Papillomavirus E8 $\wedge$ E2C proteins inhibits viral replication. *PLoS Pathogens*, **12**, e1005556.
68. Yu, F., Thiesen, J. and Strätling, W.H. (2000) Histone deacetylase-independent transcriptional repression by methyl-CpG-binding protein 2. *Nucleic Acids Res.*, **28**, 2201–2206.
69. Koerner, M.V., FitzPatrick, L., Selfridge, J., Guy, J., De Sousa, D., Tillotson, R., Kerr, A., Sun, Z., Lazar, M.A., Lyst, M.J. *et al.* (2018) Toxicity of overexpressed MeCP2 is independent of HDAC3 activity. *Genes Dev.*, **32**, 1514–1524.
70. Weissman, J.D., Howcroft, T.K. and Singer, D.S. (2000) TAF<sub>II</sub>250-independent transcription can be conferred on a TAF<sub>II</sub>250-dependent basal promoter by Upstream activators. *J. Biol. Chem.*, **275**, 10160–10167.
71. Imhof, A., Yang, X.J., Ogryzko, V.V., Nakatani, Y., Wolffe, A.P. and Ge, H. (1997) Acetylation of general transcription factors by histone acetyltransferases. *Curr. Biol.*, **7**, 689–492.
72. Choi, C.H., Hiromura, M. and Usheva, A. (2003) Transcription factor IIB acetylates itself to regulate transcription. *Nature*, **424**, 965–969.
73. Yu, J., Li, Y., Ishizuka, T., Guenther, M.G. and Lazar, M.A. (2003) A SANT motif in the SMRT corepressor interprets the histone code and promotes histone deacetylation. *EMBO J.*, **22**, 3403–3410.
74. Cowger, J.J.M. and Torchia, J. (2006) Direct association between the CREB-binding protein (CBP) and nuclear receptor corepressor (N-CoR). *Biochemistry*, **45**, 13150–13162.
75. Uthe, H., Vanselow, J.T. and Schlosser, A. (2017) Proteomic analysis of the mediator complex interactome in *Saccharomyces cerevisiae*. *Sci. Rep.*, **7**, 43584.
76. Petrenko, N., Jin, Y., Wong, K.H. and Struhl, K. (2017) Evidence that Mediator is essential for Pol II transcription, but is not a required component of the preinitiation complex in vivo. *Elife*, **6**, e28447.
77. Baptista, T., Grünberg, S., Minoungou, N., Koster, M.J.E., Timmers, H.T.M., Hahn, S., Devys, D. and Tora, L. (2017) SAGA is a general cofactor for RNA Polymerase II transcription. *Mol. Cell*, **68**, 130–145.
78. Janknecht, R., Wells, N.J. and Hunter, T. (1998) TGF- $\beta$ -stimulated cooperation of Smad proteins with the coactivators CBP/p300. *Genes Dev.*, **12**, 2114–2119.
79. Zhong, H., Voll, R.E. and Ghosh, S. (1998) Phosphorylation of NF- $\kappa$ B p65 by PKA stimulates transcriptional activity by promoting a novel bivalent interaction with the coactivator CBP/p300. *Mol. Cell*, **1**, 661–671.
80. Kamei, Y., Xu, L., Heinzel, T., Torchia, J., Kurokawa, R., Glass, B., Lin, S.C., Heyman, R.A., Rose, D.W., Glass, C.K. *et al.* (1996) A CBP integrator complex mediates transcriptional activation and AP-1 inhibition by nuclear receptors. *Cell*, **85**, 403–414.
81. Jonat, C., Rahmsdorf, H.J., Park, K.K., Cato, A.C.B., Gebel, S., Ponta, H. and Herrlich, P. (1990) Antitumor promotion and antiinflammation: Down-modulation of AP-1 (Fos/Jun) activity by glucocorticoid hormone. *Cell*, **62**, 1189–1204.
82. Ray, A. and Prefontaine, K.E. (1994) Physical association and functional antagonism between the p65 subunit of transcription factor NF- $\kappa$ B and the glucocorticoid receptor. *Proc. Natl. Acad. Sci. U.S.A.*, **91**, 752–756.
83. Kang, J.S., Kim, S.H., Hwang, M.S., Han, S.J., Lee, Y.C. and Kim, Y.J. (2001) The structural and functional organization of the yeast mediator complex. *J. Biol. Chem.*, **276**, 42003–42010.

84. Lacombe, T., Poh, S.L., Barbey, R. and Kuras, L. (2013) Mediator is an intrinsic component of the basal RNA polymerase II machinery *in vivo*. *Nucleic Acids Res.*, **41**, 9651–9662.
85. Stumpf, M., Yue, X., Schmitz, S., Luche, H., Reddy, J.K. and Borggreffe, T. (2010) Specific erythroid-lineage defect in mice conditionally deficient for Mediator subunit Med1. *Proc. Natl. Acad. Sci. U.S.A.*, **107**, 21541–21546.
86. Chen, X.F., Lehmann, L., Lin, J.L., Vashisht, A., Schmidt, R., Ferrari, R., Huang, C., McKee, R., Mosley, A., Plath, K. *et al.* (2012) Mediator and SAGA have distinct roles in Pol II preinitiation complex assembly and function. *Cell Rep.*, **2**, 1061–1067.
87. Haas, D.A., Meiler, A., Geiger, K., Vogt, C., Preuss, E., Kochs, G. and Pichlmair, A. (2018) Viral targeting of TFIIB impairs *de novo* polymerase II recruitment and affects antiviral immunity. *PLOS Pathog.*, **14**, e1006980.
88. Titov, D.V., Gilman, B., He, Q.L., Bhat, S., Low, W.K., Dang, Y., Smeaton, M., Demain, A.L., Miller, P.S., Kugel, J.F. *et al.* (2011) XPB, a subunit of TFIIH, is a target of the natural product triptolide. *Nat. Chem. Biol.*, **7**, 182–188.
89. Sato, S., Tomomori-Sato, C., Parmely, T.J., Florens, L., Zybailov, B., Swanson, S.K., Banks, C.A.S., Jin, J., Cai, Y., Washburn, M.P. *et al.* (2005) A set of consensus mammalian mediator subunits identified by multidimensional protein identification technology. *Mol. Cell*, **14**, 685–691.
90. Paoletti, A.C., Parmely, T.J., Tomomori-Sato, C., Sato, S., Zhu, D., Conaway, R.C., Conaway, J.W., Florens, L. and Washburn, M.P. (2006) Quantitative proteomic analysis of distinct mammalian Mediator complexes using normalized spectral abundance factors. *Proc. Natl. Acad. Sci. U.S.A.*, **103**, 18928–18933.
91. Yu, L., Jearawiriyapaisarn, N., Lee, M.P., Hosoya, T., Wu, Q., Myers, G., Lim, K.C., Kurita, R., Nakamura, Y., Voitek, A.B. *et al.* (2018) BAP1 regulation of the key adaptor protein NCoR1 is critical for  $\gamma$ -globin gene repression. *Genes Dev.*, **32**, 1537–1549.
92. Bhaskara, S., Knutson, S.K., Jiang, G., Chandrasekharan, M.B., Wilson, A.J., Zheng, S., Yenamandra, A., Locke, K., Yuan, J.I., Bonine-Summers, A.R. *et al.* (2010) Hdac3 is essential for the maintenance of chromatin structure and genome stability. *Cancer Cell*, **18**, 436–447.
93. Perez-Riverol, Y., Csordas, A., Bai, J., Bernal-Llinares, M., Hewapathirana, S., Kundu, D.J., Inuganti, A., Griss, J., Mayer, G., Eisenacher, M. *et al.* (2019) The PRIDE database and related tools and resources in 2019: improving support for quantification data. *Nucleic Acids Res.*, **47**, D442–D450.